

THE STUDY OF CAPILLARY ELECTROPHORESIS
— POLYIMIDES, NYLON AND NON-AQUEOUS ANALYSIS

BY

Xiaowei Sun

Dissertation Submitted for the Faculty of the
Virginia Polytechnic Institute and State University
in partial fulfillment of the requirements for the degree of

DOCTOR OF PHILOSOPHY

IN

CHEMISTRY

APPROVED



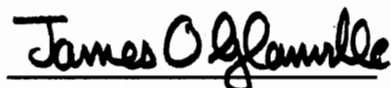
Harold M. McNair, Chairman



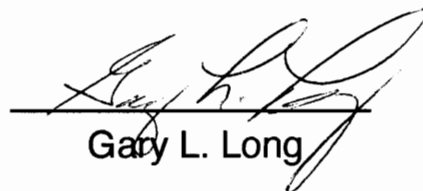
Mark R. Anderson



Harry W. Gibson



James O. Glanville



Gary L. Long

April, 1996

Blacksburg, Virginia

THE STUDY OF CAPILLARY ELECTROPHORESIS
— POLYIMIDES, NYLON AND NON-AQUEOUS ANALYSIS

by

Xiaowei Sun

Committee Chairman: Harold M. McNair
Chemistry

(ABSTRACT)

New applications of capillary zone electrophoresis (CZE) are explored. These include condensation polymer compositional analysis (1,2,3), drug in urine analysis (4) and nonaqueous CE (5) by using a mixture of N-methylformamide (NMF) and dimethylsulfoxide (DMSO).

First, the application of CZE to polyimide compositional analysis is described. The electropherograms of decomposed products from polyimide are determined by the structure of monomers from which a polyimide is made. In most cases, it is difficult to know structures for all peaks that appear in the electropherogram. But different polyimides give different patterns on the electropherogram and the same monomer in different polyimides gives a similar pattern. This pattern of electropherogram can be considered as a "finger print" of the polyimide, just as a chromatogram obtained from pyrolysis GC analysis of a polymer. It is possible to deduce the major components of the polyimide from the pattern of the electropherogram of the decomposition products of the polyimide.

Second, the application of CZE to nylon compositional analysis is studied. The hydrolysis of nylon in acidic condition gives its corresponding monomer. There is no further decomposition reaction of the monomer. This method is simple and easy. Analysis of trace amount amine impurities is possible, which is very difficult to do by other methods.

Third, a method for ranitidine, an ulcer disease, in urine is developed. Solid phase extraction conditions and the CZE procedure conditions are optimized. Experimental results show that good recovery of the drug from a urine sample and relatively good reproducibility are obtained.

Finally, non-aqueous CE using a mixture of NMF and DMSO as solvent is studied. The separation of a mixture of aromatic acids by this solvent is described.

ACKNOWLEDGMENTS

I would like to take this opportunity to express my utmost gratitude to my adviser and mentor, Dr. Harold McNair for his support, advice and patience during my study at Virginia Tech. I am grateful for the opportunity to study analytical chemistry from him and to conduct research under his guidance.

I also would like to extend my thanks to Dr. Mark Anderson, Dr. Harry Gibson, Dr. James Glanville and Dr. Gary Long for serving my committee member and their valuable help. I specially thank Dr. Glanville for the proofreading of this thesis.

My colleagues and friends at Virginia Tech also deserve my thanks. They are : Dr. Vincent Remcho, Dr. Chris Palmer, Dr. Lisa Goebel, Dr. Greg Slack, Dr. Nick Snow, Dr. Robert Klute, Dr. Maha Kahled, Dr. Yuri Kazakavich, Dr. Markus Lyman, Elena Cabasas, Yuwen Wang, Dr. Marisa Bonilla, Dr. Silvia Sargenhi, Stephanye Armstrong, Karen Baker and Gail Reed. I also thank Biao Tan for providing polyimide samples for this work.

With deepest love and appreciation, I would like to thank my parents, brothers and parents-in-law. Though thousands miles away from Blacksburg, they are constantly support, encouragement and belief in me during my study overseas, at Virginia Tech. I hope they are proud of what we have accomplished.

Most importantly, I would like to thank my wonderful wife, Xianghong, and daughter, Janet, for their unending love. I know any words are not enough in debt to them.

TABLE OF CONTENTS

	Page
Abstract	ii
Acknowledgments	iv
List of Figures	vii
List of Tables	ix
CHAPTER I. INTRODUCTION	1
1.1. Research Objectives	1
1.2. Electrophoresis	1
1.3. High Performance Capillary Electrophoresis	2
1.3.1. Capillary Zone Electrophoresis	7
1.3.2. Micellar Electrokinetic Capillary Chromatography	18
1.3.3. Capillary Isoelectric Focusing	23
1.3.4. Capillary Isotachopheresis	26
1.4. Condensation Polymer Compositional Analysis.	29
CHAPTER II. EXPERIMENTAL	32
2.1. CZE for Polyimides Analyses	32
2.1.1. Instrumentation	32
2.1.2. Chemicals	34
2.1.3. Sample Preparation	34
2.2. CZE for Nylon Composition Analysis	36
2.2.1. Instrumentation	36
2.2.2. Chemicals	36
2.2.3. Sample Preparation	37
2.3. CZE Analysis of Ranitidine in Urine Sample	39
2.3.1. Instrumentation	39
2.3.2. Chemicals and Materials	39
2.3.3. Sample Preparation	39
2.4. Non Aqueous CE	42
2.4.1. Instrumentation and Chemicals	42
2.4.2. Sample Preparation	42
CHAPTER III. RESULTS AND DISCUSSION	43
3.1. CZE for Polyimides Analyses	43
3.1.1. Properties of Polyimides	43
3.1.2. BTDA-pPDA-PA Analysis	43
3.1.3. BAPB-BPDA-PA Analysis	45

3.1.4. PMDA-DAPPO Analysis	52
3.1.5. 6FDA-DAPPO Analysis	56
3.1.6. BisA-DA-pPDA, mPDA-4-PEPA Analysis	58
3.1.7. BTDA-DAPPO Analysis	64
3.1.8. Conclusions for Polyimides Analysis	66
3.2. CZE for Nylons Analyses	68
3.2.1. Properties of Nylons	68
3.2.2. The Decomposition of Nylon by Acid	69
3.2.3. The Analysis of Nylon 6/6 and 6/9	71
3.2.4. The Analysis of Nylon 11 and Nylon 12	76
3.2.5. The Analysis of an Industrial Product	78
3.3. CZE Analysis of Ranitidine in Urine Sample	85
3.3.1. Conditions for Separation and Detection of Ranitidine by CZE	85
3.3.2. Conditions for Solid Phase Extraction	89
3.3.3. Extraction of Ranitidine from Spiked Urine Sample	95
3.4. Non Aqueous CE	99
3.4.1. N-Methylformamide as an Non Aqueous Solvent for CE Separation	102
3.4.2. The Influence of DMSO on NMF Solvent.	107
CHAPTER IV. CONCLUSIONS	109
REFERENCES	111
VITAE	116

LIST OF FIGURES

		Page
Figure 1.	Publications on Capillary electrophoresis	4
Figure 2.	Basic schematic of a CE instrument	5
Figure 3.	Electrical double layer	10
Figure 4.	The influence of pH on electroosmotic mobility	12
Figure 5.	Flow profile in HPLC and CE	13
Figure 6.	Separation in CZE with EOF.	15
Figure 7.	The interaction of solute and micelle	21
Figure 8.	A. Separation of neutral compound in MECC. B. A typical chromatogram of MECC.	22
Figure 9.	Schematic representation of the separation of CIEF	25
Figure 10.	Schematic representation of the separation of CITP	28
Figure 11.	Chromatography of nylon 6/9 and 6/10 with PY-GC-MS	31
Figure 12.	Home made CE system	33
Figure 13.	The decomposition reactions of nylon	37
Figure 14.	Schematic reactions of fluorescamine with amines	38
Figure 15.	Extraction sequences in SPE	41
Figure 16.	Fusion reaction of polyimide	44
Figure 17.	Structures of monomers for the polyimide of BTDA-pPDA-PA	47
Figure 18.	Electropherogram of polyimide sample mixture containing phthalic and terephthalic acid	48
Figure 19.	Electropherogram of polyimide sample	49
Figure 20.	Electropherogram of sample in 25 mM Na ₂ PO ₄ buffer solution	50
Figure 21.	Electropherogram of mixture of polyimide with phthalic and terephthalic acid	51
Figure 22.	The structure of BAPB, BPDA and PA	53
Figure 23.	Electropherogram of decomposed products from BAPB-BPDA-PA polyimide	53
Figure 24.	Structures of PMPA and DAPPO	55
Figure 25.	Electropherogram of the decomposed products from PMPA-DAPPO polyimide	55
Figure 26.	Structures of 6FDA and DAPPO	57
Figure 27.	Electropherogram of the decomposed products from 6FDA-DAPPO polyimide	57
Figure 28.	Structures of monomers and end cap compounds for polyimide BisA-DA-pPDA, mPDA-4-PEPA	60
Figure 29.	Electropherogram of decomposed products from BisA-DA-pPDA.	61
Figure 30.	Sample in Figure 29 spiked with end cap group	61
Figure 31.	Electropherogram of mixture in Figure 29 spiked with BisADA and end cap group	62
Figure 32.	Electropherogram of decomposed products of	

	polyimide before curing	63
Figure 33.	Electropherogram of decomposed products of polyimide after curing	63
Figure 34.	Structures of BTDA and DAPPO	65
Figure 35.	Electropherogram of polyimide BTDA-DAPPO	65
Figure 36.	Structures of nylons studied in this work	69
Figure 37.	Mechanism of amide (nylons) decomposition in acidic solution	70
Figure 38	Electropherogram of fluorescamine	75
Figure 39	Electropherogram of nylon 6/6 with fluorescamine	76
Figure 40	Electropherogram of a mixture of nylon 6/6 and 6/9 without derivatization	77
Figure 41	Electropherogram of a mixture of nylon 11 and 12 with luorescamine	79
Figure 42	Electropherogram of a mixture of nylon 6/6, 11 and 12 with fluorescamine	80
Figure 43	Separation of the industrial nylon without derivatization	82
Figure 44	Separation of the derivatives of hexamethylenediamine and BHMT with fluorescamine	83
Figure 45.	Separation of the derivative of the product	84
Figure 46.	Structure of ranitidine hydrochloride (Zantac®)	85
Figure 47.	UV spectra of Ranitidine	86
Figure 48.	Electropherogram of 100 ppm ranitidine in phosphate buffer solution	87
Figure 49.	A calibration curve of ranitidine. 8 measurements were performed for each point	88
Figure 50.	Signal to noise ratio	89
Figure 51	The influence of pH on the weight of ranitidine retained by SPE cartridge	92
Figure 52.	Electropherogram of a urine sample spiked with ranitidine before extraction	96
Figure 53.	Electropherogram of ranitidine desorption from SPE cartridge	97
Figure 54.	Electroosmotic flow in pure NMF solvent	103
Figure 55	Structures of compounds used for separation	104
Figure 56	The separation of 5 compounds in pure NMF solvent	105

LIST OF TABLES

	Page	
Table 1.	Detection Methods and Their Detection Limit in CE.	6
Table 2.	Recovery of Ranitidine from Water.	94
Table 3.	Recovery of Ranitidine from Spiked Urine.	98
Table 4.	Physical Properties of Some Organic Solvents for CE	101
Table 5.	The Influence of %DMSO (v/v) on the Electrophoretic Mobility of Analytes.	106
Table 6.	The Efficiency, Reproducibility in Migration Time and Peak Area of Analytes in NMF solvent.	108

CHAPTER I. INTRODUCTION

1.1. Research Objectives

Capillary electrophoresis (CE) is a rapidly developing technique. Much of the recent focus in CE has been, and will continue to be, on the methods development and the application of CE to a variety of modern-day analytical problems. The work here focuses on new applications of capillary zone electrophoresis (CZE). The objectives have been: (1) to develop a simple and easy method for condensation polymer compositional analysis by CZE (for nylon and polyimides); (2) to develop a method for drug analysis in urine and; (3) to study nonaqueous CE analysis by using a mixture of DMSO and N-methylformamide.

1.2. Electrophoresis

Electrophoresis and chromatography are the most widely used techniques of separation science in modern analytical chemistry.

In chromatography, a gas or liquid passes through a column packed (or coated) with a stationary phase. The separation of analytes results from the differences in the free energy of partitioning of analytes between the two phases.

In electrophoresis, the driving force is an applied electric field. Charged species move in a fluid under the influence of an applied electric field. The separation is based on the different ratios of net charge to molecular size. This

technique is widely used by biochemists for the separation of mixtures of nucleic acids, peptides, and proteins (6). The separation is carried out in a medium such as slab gel, paper or agarose. Such media not only provide physical support and mechanical stability for the mobile buffer solution, but also perform other important functions, such as molecular sieving and reduction of diffusion and convection.

1.3. High Performance Capillary Electrophoresis

Capillary electrophoresis (CE) is a relatively new and a rapidly growing analytical technique. A major limitation in normal electrophoretic techniques is solution heating (or Joule heating) due to the ionic current carried between the electrodes. Joule heating can affect electrophoretic mobilities, increase zone broadening, and decrease separation efficiencies. A unique advantage of capillary tubes is the enhanced heat dissipation due to the large surface area to volume ratio of the capillary. Large inner surface area to volume ratios in small bore capillary tubes provide more efficient heat dissipation relative to large scale systems.

Virtanen (7) is one of the earliest workers to small diameter Pyrex™ tubing (200 to 500 μm) for free zone electrophoresis. He analyzed the cations Li⁺, Na⁺ and K⁺ in 1974. He also mentioned the importance of electroosmotic flow as a factor on the electrophoretic behavior of an analyte. In 1979, Everaerts et al.(8) explored the separation potential of capillary zone electrophoresis (CZE) in a 200 μm Teflon capillary with on line UV detection . And in 1981, Jorgenson and co-workers were the first to demonstrate that the

use of even narrower capillaries (< 100 μm ID) produces highly efficient electrophoretic separations (9,10). These authors gave a brief description of some of the theoretical aspects of CE and showed that electroosmosis played an important part in determining the mobility of ionic species. Since their work, the publications and reviews of CE have risen dramatically (Figure 1).

The instrumentation for CE is simple. Figure 2 is a schematic diagram of a typical CE system. There are three main parts: high voltage power supply, separation column, and detector. The power supply operates up to 30 kV and is connected to two platinum electrodes which are dipped in buffer solutions. The ends of the capillary column (fused silica with lengths from 20 - 100 cm and internal diameter of 25 - 100 μm) are also dipped into the buffers. The detector is placed between the two ends of the column where an optical window is created by burning off about 2 mm of the polyimide coating.

Almost all the detectors used in HPLC are now used in CE. They are UV detectors (including photodiode array [PDA]) (11-3), fluorescence (including laser induced fluorescence) (14-17), amperometric (18), conductivity (19), Raman (20), radiochemical(12), mass spectroscopy (22-26) and indirect detection (27-29). The development of CE-MS will have a great impact on the application of CE. Table 1 shows the detection modes and their detection limits presently available in CE(18).

Over the past 15 years, several modes of CE have been developed. They are: (1) capillary zone electrophoresis (CZE); (2) micellar electrokinetic capillary chromatography (MEKC); (3) capillary isotachopheresis (CITP) and; (4) capillary isoelectric focusing (CIEF)

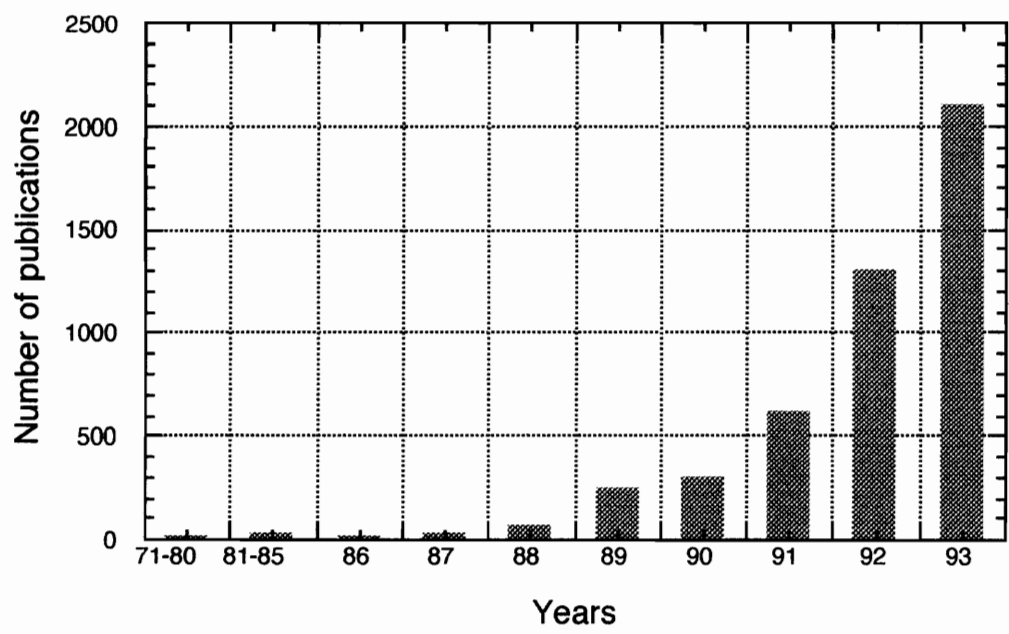


Figure 1. The growth of publications on Capillary Electrophoresis from 1971 to 1993. (J. P. Landers, Ed., Handbook of Capillary Electrophoresis, CRC Press, 1994, p 11.)

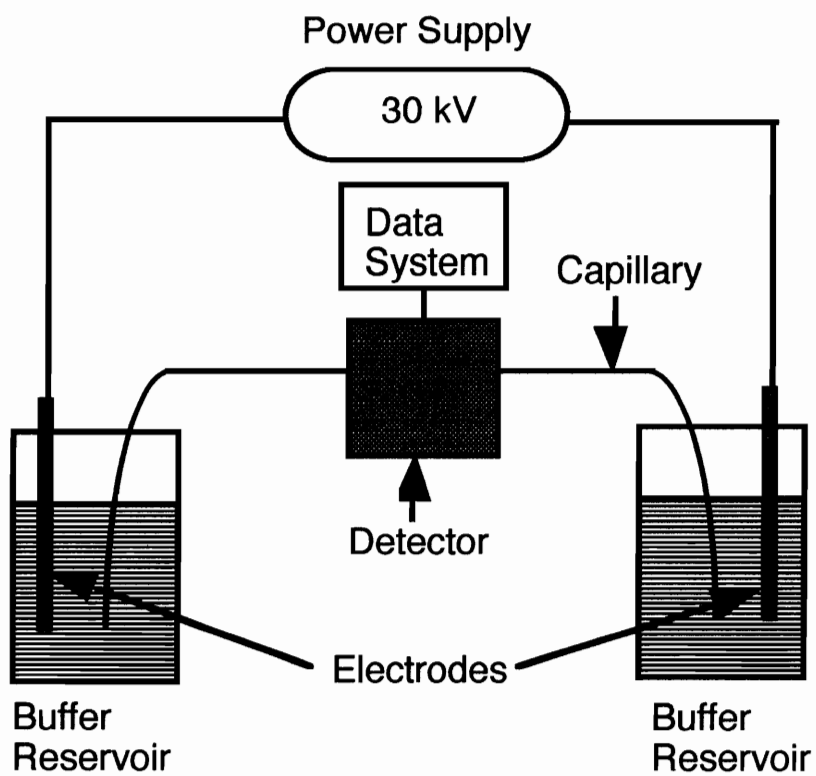


Figure 2. Basic schematic of a CE instrument.

Table 1. Detection Methods and Their Detection Limits in CE.

<u>METHOD</u>	<u>DETECTION LIMIT (moles)</u>
UV-Vis absorption	10^{-13} - 10^{-15}
Fluorescence (laser induced fluorescence)	10^{-17} - 10^{-20}
Mass spectrometry	10^{-17}
Amperometry	10^{-19}
Conductivity	10^{-16}
Raman	10^{-15}
Radiometry	10^{-19}

1.3.1. Capillary Zone Electrophoresis

Capillary zone electrophoresis (CZE) is the simplest and also the most used CE mode. CZE has been used in the analysis of a wide range of charged simple inorganic ions (30,31), organic molecules (32-34), chiral compounds (35,36), peptides (37-39), and proteins (40-43).

Separation in CZE is based on the relative mobility of the analytes. Mobility of ions in solution depends on their charge/size ratio. The size of the molecule is based on the molecular weight, the three dimensional structure and the degree of solvation.

According to Coulomb's law, an ionic sample is accelerated by an electric force F_e :

$$F_e = qE \quad (1)$$

Where q is the net charge of the ion and E is the strength of electric field. This force causes the movement of ions toward the opposite charged electrode. As the velocity of the ions increases, the frictional force (F_f) caused by the viscous drag of the surrounding solution slows down the ions. For a spherical molecule, this force can be expressed in terms of Stokes' law as:

$$F_f = 6\pi\eta r v_{ei} \quad (2)$$

Where η is the viscosity of the solvent medium, r is the radius of the solvated ion and v_{el} is the velocity of ion. Since $F_f = F_e$, equations 1 and 2 can be rearranged to:

$$v_{el} = qE/6\pi\eta r \quad (3)$$

Thus, the viscosity of the solvent, the net charge, and actual size of the ions control the migration of a species in an applied electric field.

The mobility of the ion can also be expressed as:

$$\mu = v_{el}/E = q/6\pi\eta r \quad (4)$$

Equation (4) shows the important role of solvent viscosity on electrophoretic mobility. Viscosity is temperature dependent, which means that temperature control is very important for reproducibility in capillary electrophoresis experiments.

In CZE analysis, cations, which are introduced into the positive end of the capillary, should move toward the cathode and should be separated according to their q/r ratio. Neutral species should show no movement and anions should migrate electrophoretically towards the anode. However, both anions and neutrals also move towards the cathode due to the strong electroosmotic flow occurring inside the capillary.

Electroosmotic flow (EOF) originates from the electrophoretic movement of the hydrated part of the electric double layer at the capillary wall. The fused silica surface is negatively charged at $\text{pH} > 2$ due to the presence of ionized

silanol groups (44). An anionic charge on the capillary surface results in the formation of an electric double layer. Figure 3 shows the ionic distribution in the solution. Anions are repelled from the negatively charged wall region, whereas cations are attracted as counterions. Ions closest to the wall are tightly bound and immobile; this region is called the Stern layer. Further from the wall is a compact and mobile region with substantial cationic character, which is called the Gouy-Chapman layer or diffusion layer. The thickness of the diffusion layer is less than 100 nm, depending on ionic strength, type and pH of buffer and the surface of the capillary column. At a further distance from the wall, the solution becomes electrically neutral.

When an electric field is applied, the diffusion layer (with excess cations) migrates towards the cathode. Due to the viscosity of the solution, the fluid in the buffer is mobilized as well. The electroosmotic flow as defined by Helmholtz-Smoluchowski in 1903 is given by:

$$v_{eo} = E\zeta\varepsilon/\eta \quad (5)$$

where ε is the dielectric constant, η is the viscosity of the buffer and ζ is the zeta potential of the liquid-solid phase interface. Electroosmotic mobility can be expressed as:

$$\mu_{eo} = \zeta\varepsilon/\eta \quad (6)$$

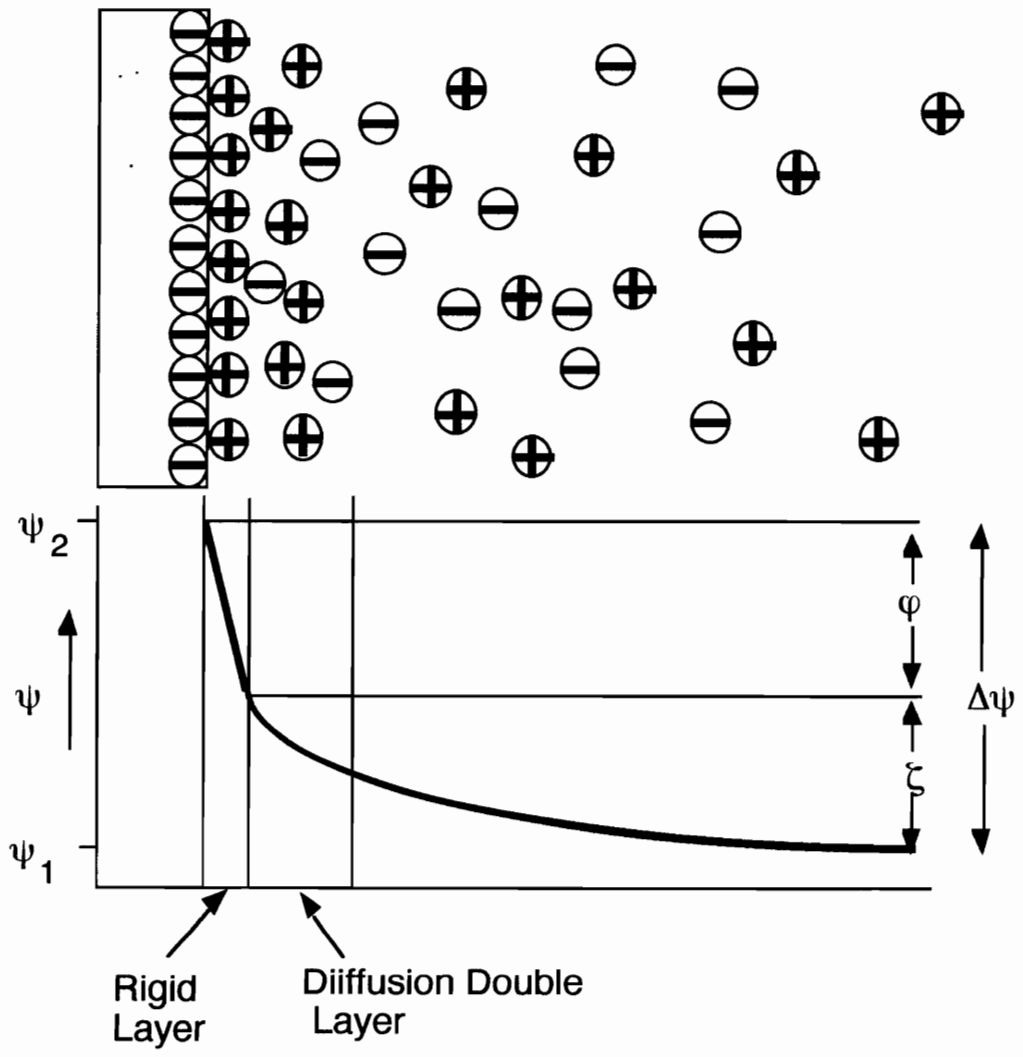


Figure 3. Representation of the electrical double layer versus distance from the capillary wall.

From equation 6 it can be seen that dielectric constant, viscosity of the solution, and the zeta potential on the surface of capillary wall govern the magnitude of electroosmotic flow. The change of dielectric constant and viscosity is not so significant for a solution when pH or composition changes. The zeta potential is determined by the charge density on the surface of the capillary. The latter is greatly influenced by the pH of the buffer. So the pH of the buffer has a great influence on the value of EOF. Their relationship is shown in the Figure 4.

A important feature of the electroosmotic flow is its flow profile. Unlike the parabolic hydrodynamic flow generated by pressure (HPLC, GC, etc), EOF is almost pluglike, and does not significantly contribute to the dispersion of zones during the separation (Figure 5). It is this plug flow profile and the lack of a stationary phase that results in the extremely high efficiency (1 million theoretical plates) (45). When no electroosmotic flow occurs, (only electrophoretic), ion movement will still be pluglike.

The separation by CZE can be achieved with and without EOF. When the surface of the capillary is coated with a layer to reduce the zeta potential, there is a little or no EOF (46-48). In this situation, separation is based solely on the differences in the electrophoretic mobilities of analytes. For protein analyses, the capillary wall usually needs to be coated with a hydrophobic layer to eliminate the interactions (adsorption) between the proteins and the capillary wall. Such interactions will result in peak tailing or even irreversible adsorption of protein molecules to the capillary wall.

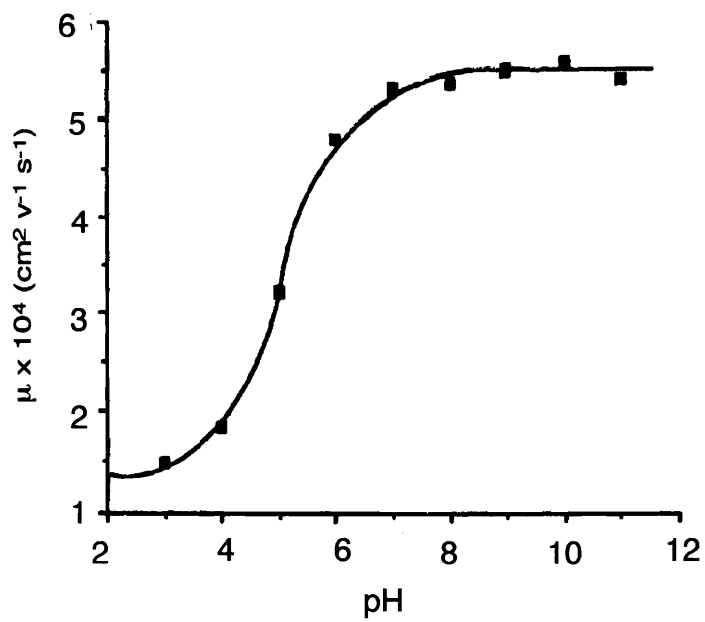


Figure 4. The influence of pH on electroosmotic mobility in fused silica⁽⁶⁹⁾.

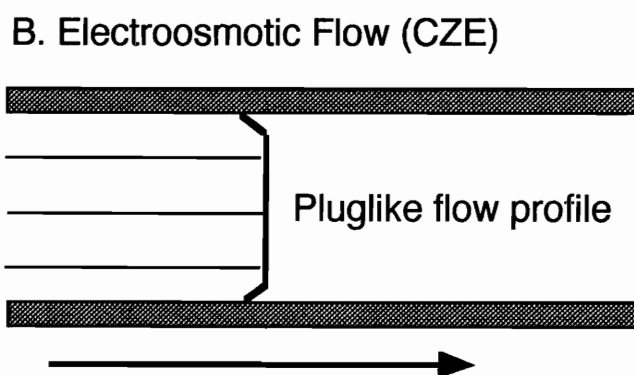
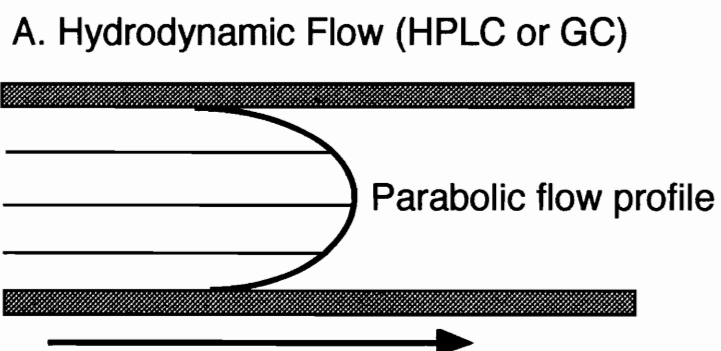


Figure 5. Flow profiles in HPLC and CE.

With electroosmotic flow, the separation of both cations and anions in a single run is possible, provided that the electroosmotic mobility is higher than anion electrophoretic mobility and that the ions do not adsorb to the capillary wall. The separation in EOF is shown in Figure 6. The net velocity of a solute v_{net} is:

$$v_{net} = v_{eo} + v_{el} \quad (7)$$

All neutrals are transported by electroosmotic flow and not separated by CZE since their q/r ratio is zero. In order to separate neutrals, additives such as surfactants would have to be included in the buffer to affect some type of partitioning. This type of CE is known as micellar electrokinetic capillary chromatography (MEKC or MECC).

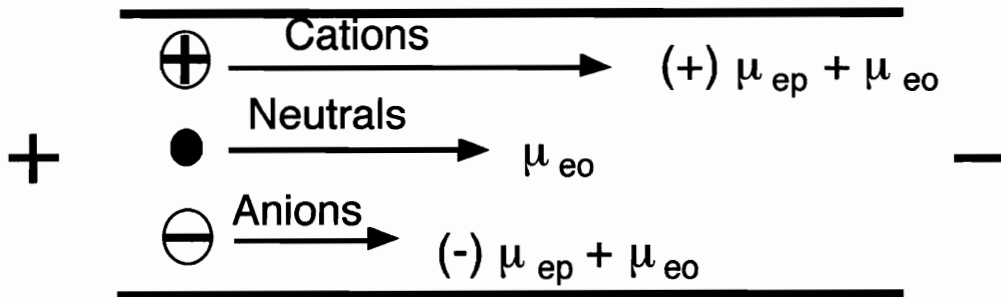
The separation theory, efficiency and resolution calculations of CZE is briefly discussed by Jorgenson and Lukacs (9), assuming that molecular diffusion is the only source of band broadening. Diffusion of ions in solution can be expressed by the Einstein equation as:

$$\sigma_x^2 = 2 D_a t \quad (8)$$

where D_a is the diffusion coefficient of the solute in buffer solution, σ_x is the diffusion, and t is the time the solute stays in the solution. The column efficiency, measured in terms of theoretical plates N , is given by Giddings:

$$N = L^2/\sigma_x^2 = L^2 / 2 D_a t \quad (9)$$

A. Vector Sum of Electroosmotic and Electrophoretic Velocity



B. Typical Electropherogram

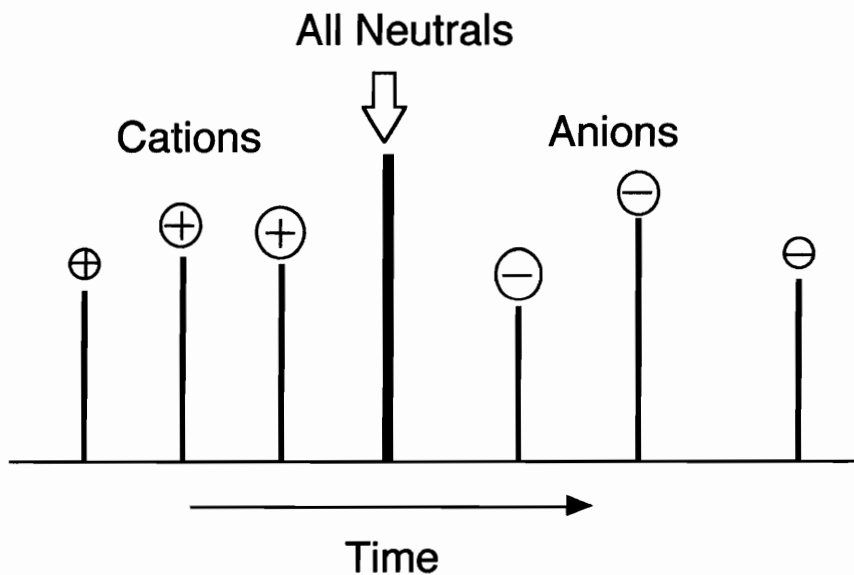


Figure 6. Separation in CZE with EOF.

When electrophoretic and electroosmotic velocities are considered equation 9 can be written as:

$$N = (\mu_{eo} + \mu_{el})VL_d/L_t2D_a \quad (10)$$

where V is the voltage applied to the capillary column, L_d is the column length to the detector, L_t is the total length of the column and D_a is the diffusion coefficient of the species in the running buffer at the column temperature. The higher the electric field, the less time the analyte will spend in the column and the less time that will be available for diffusion. So fast separations lead to high efficiency. However, the electric field cannot be taken to extremely high levels because of Joule heating (49). As a consequence of Joule heating, a temperature difference between the center and the wall of the capillary is established. That results in band broadening due to the different migration rates across the capillary diameter (50). The voltage used in CZE is determined by several parameters, such as capillary length, internal diameter, type of buffer, buffer concentration and the efficiency of capillary thermostating or cooling. In the real world, the maximum voltage that can be applied without producing a significant heat problem for a buffer is determined by Ohm's law plot (51,52).

The resolution (R_s) in CZE can be expressed as: (4)

$$R_s = \frac{N^{1/2}}{4} \frac{\mu_1 - \mu_2}{\mu_{avg} + \mu_{eo}} \quad (11)$$

From this equation, it can be seen that resolution increases with column length. Resolution also increases when the difference in electrophoretic mobilities between two analytes increases. This can sometimes be achieved by manipulating the pH of the solution. Maximum resolution is obtained when $\mu_{e0} = -\mu_{avg}$, but at this condition the analysis time approaches infinity.

1.3.2. Micellar Electrokinetic Capillary Chromatography

As mentioned previously, CZE cannot separate neutral molecules. In 1984, Terabe et al. ⁽⁵³⁾ introduced the use of ionic surfactant micelles in the buffer solutions to separate neutral molecules. This mode of CE is called micellar electrokinetic capillary chromatography (MEKC or MECC). MECC allows neutral and charged solutes to be separated simultaneously with a CZE instrument.

A surfactant consists of amphiphilic molecules, each with a hydrophobic tail and an ionic head group. Above a certain concentration, known as the critical micelle concentration (CMC), surfactants form roughly spherical and dynamic aggregates that are at equilibrium with the monomer surfactant molecules in the solution. The CMC value depends on the type of surfactant and other parameters such as temperature, pH, ionic strength of the solution, as well as the presence of organic solvents. The average number of monomers per micelle differs according to the monomer structures ⁽⁵⁴⁾. In aqueous solutions, micelles are oriented so that their hydrophilic part is on the surface of the micelle and hydrophobic moiety is in the interior. Micelle numbers increase with an increase in surfactant concentration.

Solutes present in the micellar solution will partition between the micelles and the solution. Three types of interactions may occur, depending on the hydrophobicity and hydrogen bonding capability of the solute ⁽⁵⁵⁾. Figure 7 schematically shows these types of interactions.

MECC is most commonly performed with anionic surfactants, especially sodium dodecyl sulfate (SDS). There are two phases in the MECC solution: aqueous and micelle. SDS micelles have negative charges on the surface and

have their own electrophoretic mobilities in solution. The net mobility of a micelle will be $\mu_{mc} = \mu_{e0} - \mu_{ep}$. When the electroosmotic flow (μ_{e0}) is larger than the electrophoretic mobility (μ_{ep}) of micelles, the micelles will move in the same direction as the whole solution. Analytes will distribute themselves between the micellar and the aqueous phases. When the analyte is partitioned inside the micelle, it moves with the same speed as the micelle (μ_{mc}). Otherwise it moves at the speed of bulk solution (μ_{e0}). Analytes are separated by the difference in their partitioning into the hydrophobic micelle. Extremely polar solutes will not interact with the micelles; they will elute with the electroosmotic flow at t_0 . On the other hand, extremely hydrophobic solutes will have strong interactions with the micelle and will stay essentially within the micelles at all times. The elution time of this compound can be regarded as a marker for determining the migration time of micelles, t_{mc} . Other compounds which are between these two extremes will elute within a window determined by t_0 and t_{mc} . However, this elution window is considered a major drawback for MECC since only limited peak capacity is available within this migration window (Figure 8).

In order to overcome this drawback, several creative methods have been explored to improve selectivity of the micelles, including the addition of metal ions (56), mixed surfactants (57,58) and non-ionic surfactant like Brij 35 (59). Oligomeric sodium undecylenate was specifically synthesized for MECC to tolerate high concentrations of organic modifier (60). Chiral surfactants have been synthesized for chiral separations (61-63). MECC shows both faster and easier separation of chiral compounds, compared to HPLC, due to the high

column efficiencies (N). Attempts to synthesize new chiral functional polymers for chiral separations has been carried out in this laboratory.

Several review articles and book chapters on MECC give more detailed theories of MECC, methods development and applications (64-67). Note that since MECC uses two phases, it is a form of chromatography and the results are called chromatograms, not electropherograms.

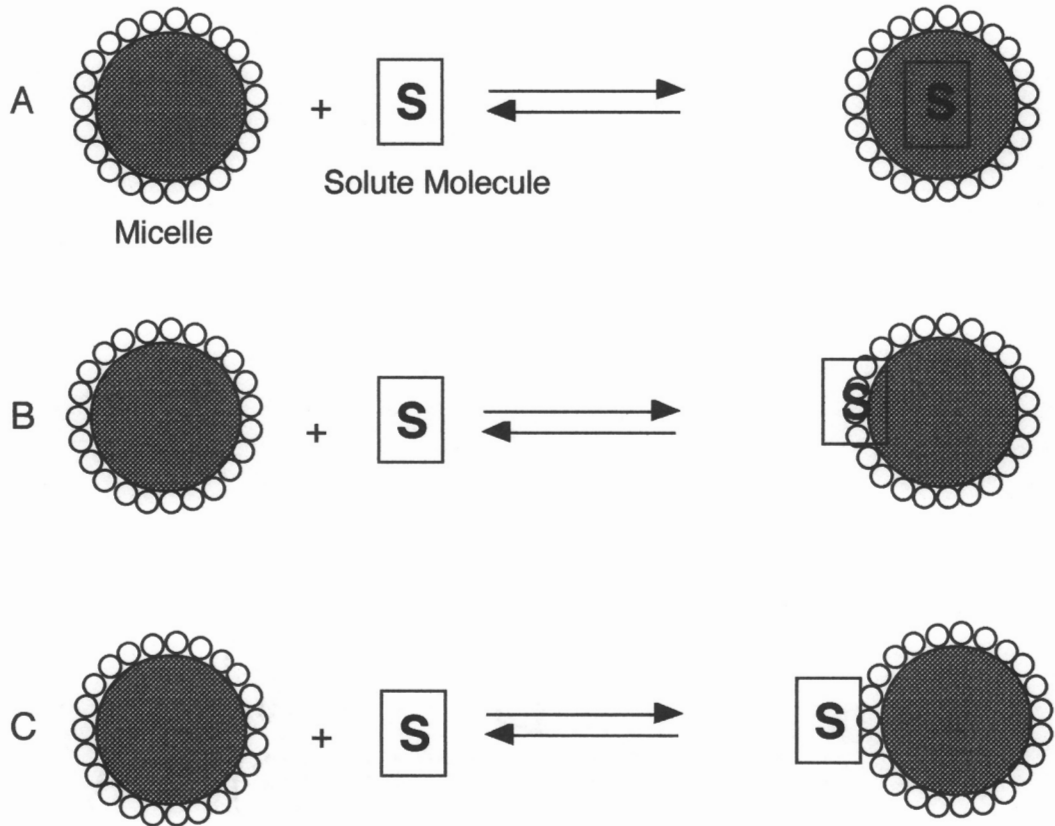


Figure 7. The interaction of a solute and a micelle may be a result of any of the above forms. A. partitioning into the interior of micelle. B. partitioning with the surface of the micelle. C. surface interaction with the head group of the surfactant monomer.

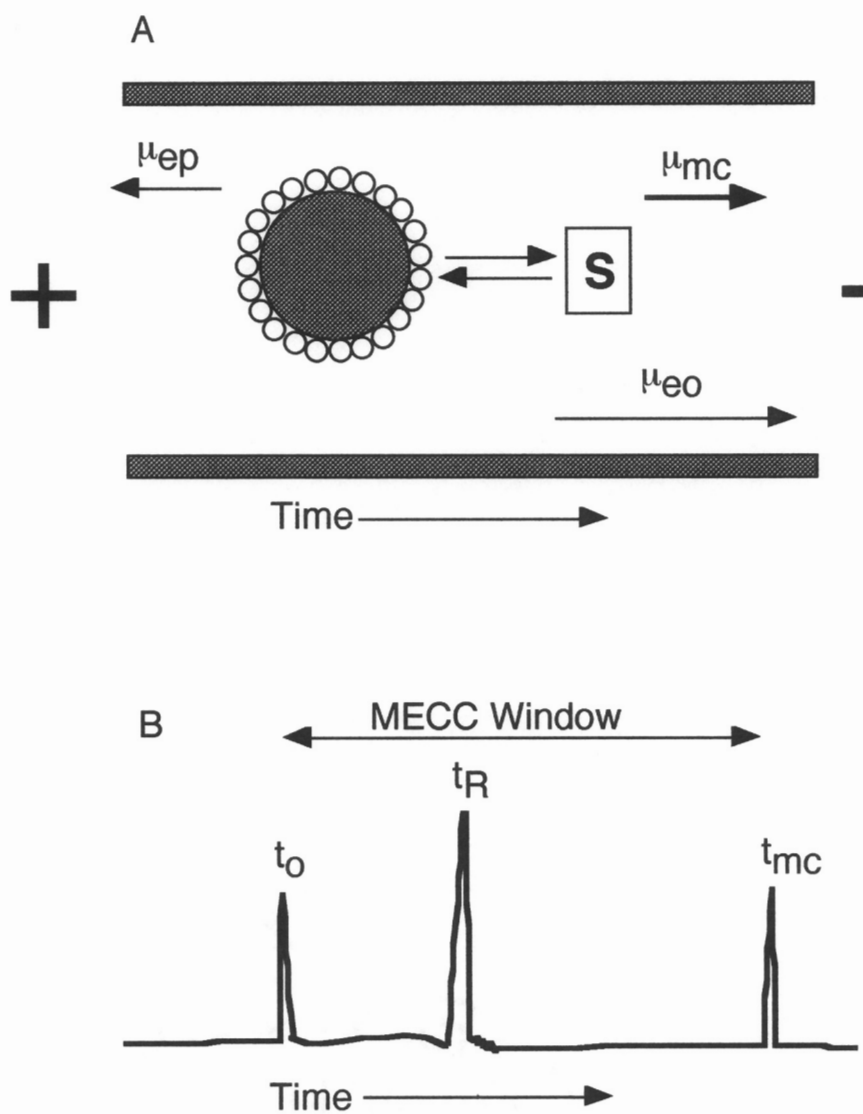


Figure 8. A. Separation of neutral compounds by MECC.
 B. A typical chromatogram in MECC.

1.3.3. Capillary Isoelectric Focusing (CIEF)

Isoelectric focusing is used to separate amphoteric molecules (like proteins). The separation is not based on the differences in net mobility as in CZE, but is based on the differences in their isoelectric points (pI) (69). A pI is that pH at which an ampholyte has zero net charge. At pI the ampholytes are present in their Zwitterionic form and do not migrate under an applied electric field. At lower pH, they are positively charged and will migrate toward the cathode. At pH higher than their pI, they are negatively charged and will migrate toward the anode. Conventional isoelectric focusing is performed in a support medium such as a slab gel. In capillary isoelectric focusing (CIEF), the separation is performed in free solution, but the capillary is coated to reduce the electroosmotic flow. *Mobilization* was introduced by Hjerten and Zhu's work to force the proteins to move past the detector window (70).

To perform a CIEF experiment, the sample is mixed with carrier ampholytes, which are commonly a mixture of polycarboxylic acids, and loaded into a coated capillary column (Figure 9) (71,72). The column is dipped in two buffer reservoirs; the anode reservoir is filled with acidic solution (low pH) and the cathode contains basic solution (high pH). When the experiment is started, cations migrate to the cathode and anions migrate to anode. The ampholytes migrate according to their charge and pI towards the corresponding electrodes and neutralize the migrating protons and hydroxyl ions. As the focusing proceeds, a pH gradient forms, and the solutes migrate to appropriate positions where the pH is equal to their pI. After focusing, the contents of the capillary are mobilized to move past the detector in order to record the electropherogram. There are three ways to accomplish the mobilization; (1) salt

mobilization ⁽⁷³⁾, (2) hydrodynamic mobilization ⁽⁷⁴⁾ and (3) electrophoretic mobilization. CIEF is mostly used for proteins separations.

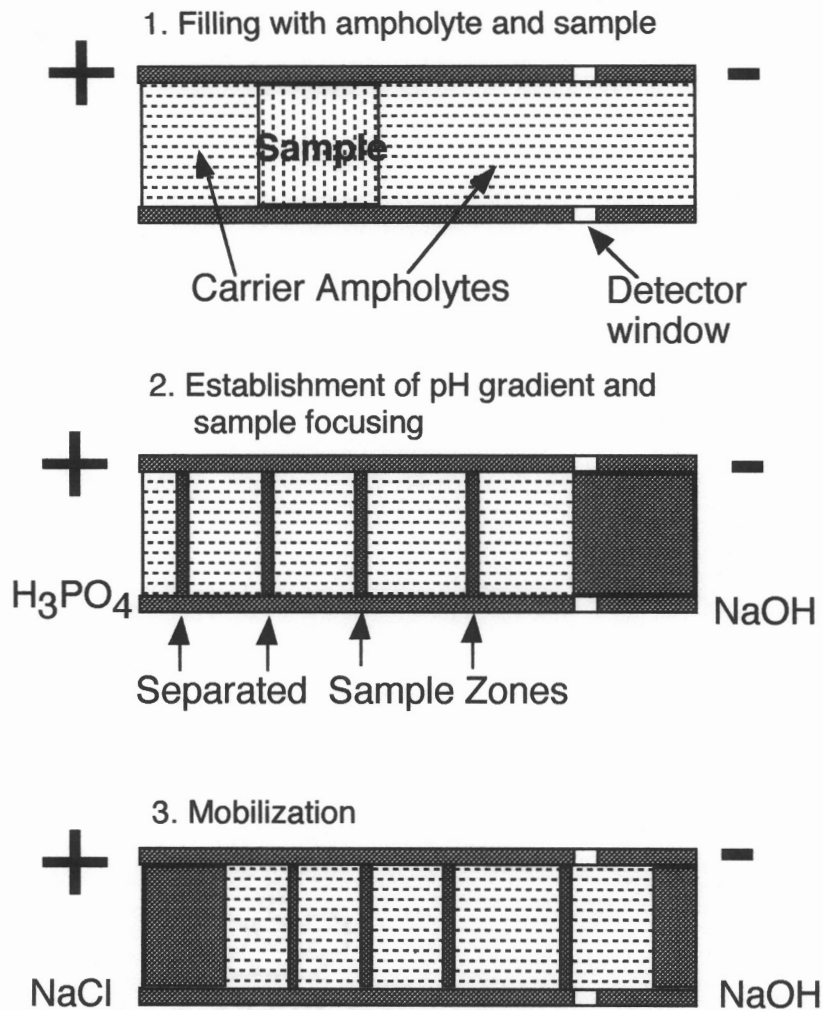


Figure 9. Schematic representation of the separation by CIEF

1.3.4. Capillary Isotachopheresis (CITP)

Isotachopheresis (ITP) literally means “electrophoresis at uniform speeds”. This means that all sample zones migrate with the same electrophoretic velocity when a steady state is established.

The separation by capillary isotachopheresis (CITP) is illustrated in Figure 10. The capillary and the detector side buffer reservoir are filled with a leading electrolyte, which has a mobility greater than that of any of the components to be separated. The sample is then loaded into the other side of the column. The column is filled with a terminating electrolyte, which has a mobility less than that of the components in the sample. As the voltage is applied, individual solutes begin to migrate at their own mobilities. As the bands begin to separate, the field strength over each sample zone changes. At equilibrium, the isotachoelectrophoretic velocity for each component can be expressed as:

$$V_{ITP} = V_L = V_A = V_T \quad (12)$$

or

$$V_{ITP} = E_L \mu_L = E_A \mu_A = E_T \mu_T \quad (13)$$

where L represents the leading electrolyte, A is the analyte and T is the terminating electrolyte. At the steady state, all zones move at the same speed

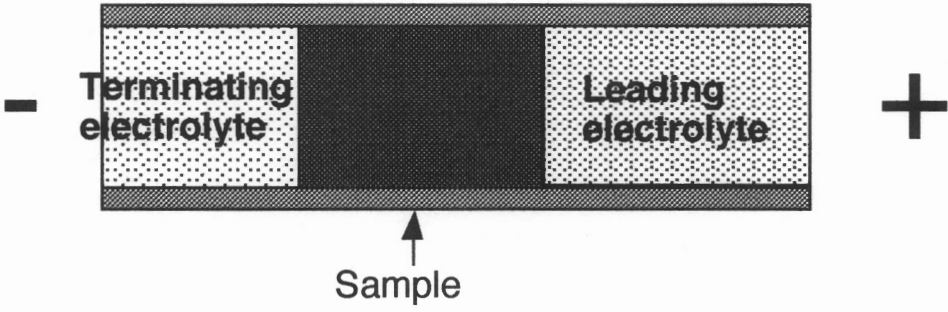
(V_{ITP}). The concentrations of all zones are related to the concentration of the leading electrolyte. It is expressed as (75):

$$C_i = C_L \frac{\mu_i(\mu_L + \mu_C)}{\mu_L(\mu_i + \mu_C)} \quad (14)$$

where C_i is the analyte concentration at steady state; C_L is the concentration of the leader; and the mobility terms are for the analyte, leader and counter ion of leader.

One important characteristic feature of CITP is trace enrichment. When the concentration of the leader is higher than the solutes concentration, zone compression occurs because of the high field strength generated over the diluted zone. This property is employed in CZE for trace analysis; the sample is first enriched by CITP and then separation is carried out by CZE (76-78). CITP is used for both proteins and nucleosides analysis (79-81).

A. Filling with leading electrolyte,
sample and termination electrolyte



B. At the steady state

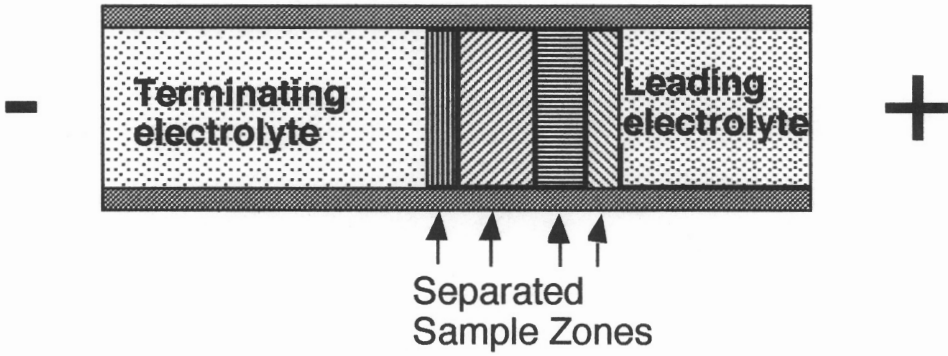


Figure 10. Schematic representation of the separation of CITP

1.4. Condensation Polymer Compositional Analysis

The analysis of polymers is associated with techniques such as infrared spectroscopy (IR), nuclear magnetic resonance (NMR), pyrolysis gas chromatography with mass spectrometry (PY-GC-MS) and size exclusion chromatography (SEC). When a new material appears, some people always want to know what it is made from. In the terms of chemistry, what are the components of the material and what is their ratio?

IR spectroscopy is the first choice to study polymers (82). It is widely available and easy to operate. IR spectroscopy also provides valuable information on the functionality of polymers. However, this technique is most used to characterize pure compounds, and it is unsuitable for the complete examination of many polymer systems due to its low sensitivity and low discriminating power for complex polymers.

NMR spectroscopy is another powerful technique to analyze polymers (83). It not only provides the structures of monomers, but also provides other important information such as microstructure and morphology of the polymer. But this technique is limited by its availability for routine analysis and the need for an experienced person to explain the results. This technique is also unsuitable for trace impurities analyses due to its limitations in sensitivity.

The unique advantage of GC is its ability to rapidly separate and detect extremely complex and small quantities of compounds. GC has long been used for polymer analysis, such as to detect residual solvents, monomers, additives like antioxidants, and ultraviolet absorbents. GC is also used for polymer compositional analysis. Before injection into a GC, the polymer is decomposed,

either on line or off line, at high temperature. One example of this technique is pyrolysis GC, which is widely used to perform the polymer compositional analysis (84). However a limitation of this method is that too many fragments are formed by pyrolysis to do the trace impurities analysis. Figure 11 shows a chromatogram of PY-GC-MS of nylon 6/9 and 6/10. Another limitation of GC is that only volatile compounds can be analyzed. This sometimes limits the GC's ability to do complete compositional analysis for polymers, for example when nonvolatile products are produced.

Fusion reaction chromatography, which was named by Haken and co-workers (85), is a powerful analytical tool for condensation polymers. In this technique, a condensation polymer is decomposed to its corresponding monomers by acids or bases, often at high temperature. Decomposition products are then separated by extraction or other methods and derivatized with appropriate reagents. Finally, the derivatives are analyzed by GC or HPLC. The beauty of this technique is the complete analysis of all the reaction products. The disadvantage of this method is that it is time-consuming and that tedious procedures such as separations and derivatizations are often necessary for condensation polymer analyses.

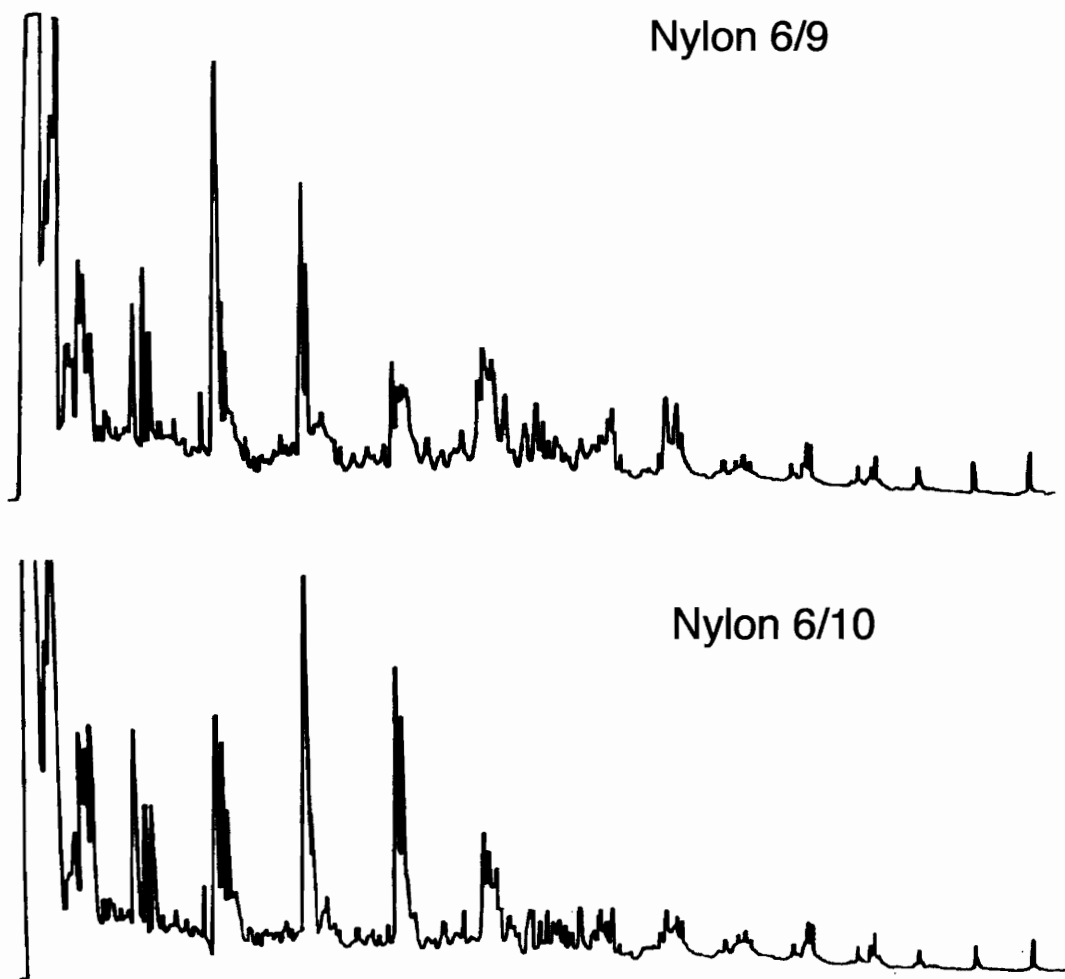


Figure 11. Chromatography of nylon 6/9 and 6/10 with PY-GC-MS (84).

CHAPTER II. EXPERIMENTAL

2.1. CZE for Polyimides Analyses

2.1.1. Instrumentation

The instrumentation used for this work was a home made system. It is shown in Figure 12. A Spellman CZE 1000R (High Voltage Electronics Corporation, Plainview, NY) was used as a high voltage source and a Model 200 variable wavelength HPLC detector (Linear Instruments Corporation, Reno, Nevada) was used as an on-line detector. Data were recorded on a Hewlett-Packard model 3390A integrator (Hewlett-Packard, Avondale, PA). A plexiglass box with a safety interlock was placed at the anode end to protect the operator from high voltages.

Fused silica capillary columns with 75 μm inner diameters and 350 μm outer diameters were obtained from Polymicro Technologies (Phoenix, Arizona). A window was made by burning off about 3 mm of polyimide coating on the capillary for on-line detection. The capillary column was installed in the UV detector by aligning the window in the optical path of the detector. The new capillary column was conditioned by flushing with 0.1 M NaOH for 15 minutes, followed by 0.01 M NaOH for another 15 minutes and then by deionized, double distilled water for 5 minutes. Finally, it was conditioned by running the operating buffer for 10 minutes before injection of any sample. Between runs, the column was rinsed with 0.01 M NaOH for 2 minutes, deionized, double distilled water for 5 minutes, and running buffer for 5 minutes. All these washes

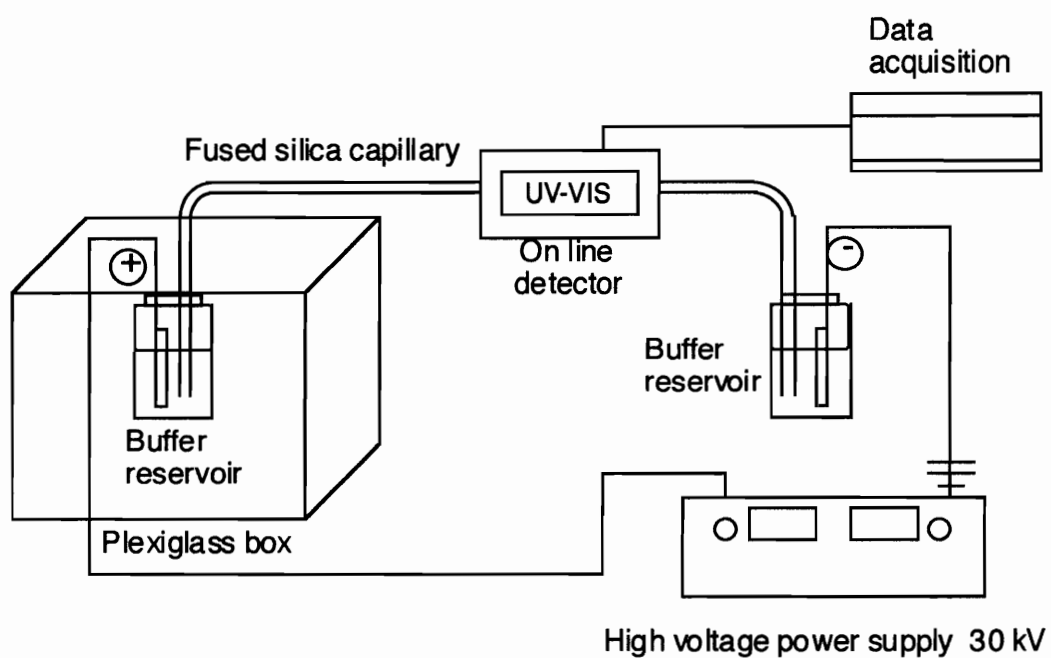


Figure 12. A schematic diagram of home made CE system used in this research.

were achieved by applying a low vacuum by aspirating on one end of the column while the other end of the column was immersed in the appropriate solutions. For overnight storage, air was first flushed through the capillaries to prevent formation of a gel layer inside the capillary ⁽⁸⁶⁾.

2.1.2. Chemicals

Potassium hydroxide, sodium acetate, phosphoric acid, boric acid and sodium phosphate were purchased from Aldrich (Milwaukee, WI). Polyimide samples were synthesized at Virginia Tech and were generously provided by Mr. Biao Tan of the Chemistry Department for this research.

2.1.3. Sample Preparation

Borate buffer (75 mM and pH = 9.2) was prepared as follows: dissolving 0.9275 grams of boric acid in 150 mL of deionized, double distilled water, then adjusting the pH of the solution with 1 M NaOH to 9.2; finally diluting the solution to 200 mL with deionized double distilled water. Phosphate buffer (pH = 8.2) was prepared by adding 50 mM H₃PO₄ to 50 mM K₃PO₄ in water to reach pH=8.2. All solutions were filtered through 0.45 mm nylon filters (Supelco, Bellefonte, PA) before use.

Polyimide (20 mg) was mixed with 200 mg potassium hydroxide and 5 mg sodium acetate. The mixture was sealed in a glass tube (15cm x 0.5cm) under vacuum. The reaction was carried out at 250°C for 45 minutes. Afterwards, the glass tube was cooled to 0°C before opening to prevent

evaporation of the diamine. The reaction mixture was dissolved in 5 mL of distilled water. One mL of the solution was filtered through a 0.45 μm nylon filter (Supelco, Bellefonte, PA). The pH of the filtered solution was adjusted to 8.5 using dilute HCl.

2.2. CZE for Nylon Composition Analysis

2.2.1. Instrumentation

Two instruments were employed in this part of the work. The first was the home made system which was previously described. The second was a Beckman P/ACE System 2100 instrument (Beckman, Fullerton, CA). This second system comprised a selectable wavelength UV detector, the GOLD software for control and data collection, and a 0 - 30 kV high voltage power supply. The capillaries are housed in a cartridge and the temperature of the column is controlled by a fluorocarbon cooling fluid. In all experiments, the temperature was set at 22 °C. All the electropherograms were collected by an IBM PS/2 Model 55 SX computer.

2.2.2. Chemicals

Hydrobromic acid (47% - 49%) was purchased from J. T. Baker (Phillipsburg, NJ). Polyamides, potassium hydroxide, sodium acetate, boric acid, hydrobromic acid and sodium phosphate were purchased from Aldrich Chemical Company (Milwaukee, WI). Acetone was purchased from EM Science (Cherry Hill, NJ). Fluorescamine was purchased from Sigma Chemical Co. (St. Louis, MO).

2.2.3. Sample Preparation

The borate buffer preparation was described earlier.

Acetone solution of fluorescamine (2 mg/mL) was prepared by dissolving 20 mg fluorescamine in 10 mL acetone and storing at room temperature.

Into a reaction tube, 20 mg of polyimides and 1 mL of hydrobromic acid were added. The reaction tube was capped and heated to 120°C for one hour. The decomposition reaction is shown in Figure 13. After reaction, excess hydrobromic acid was removed by purging with nitrogen and the pH of the solution was adjusted to 9 with 1.0 M NaOH. The solution was filtered through a 0.45 μm nylon filter and diluted to 10 mL with deionized water.

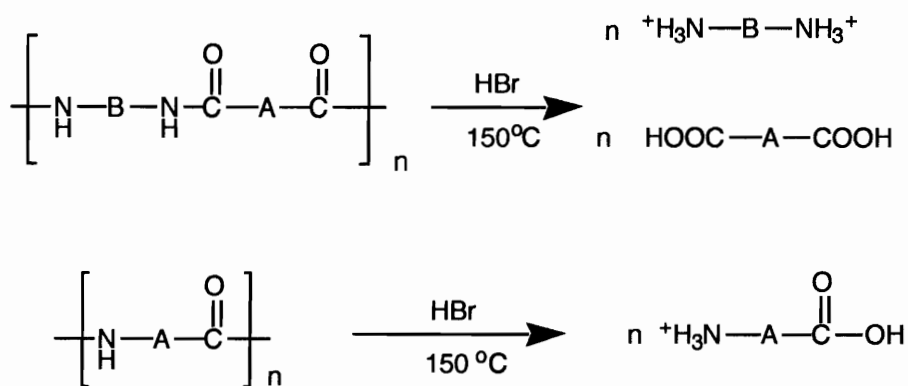


Figure 13. The decomposition reactions of nylon in acidic condition.

The derivatization of amines with fluorescamine was as follows; into a 4.5ml sample vial (Beckman, Fullerton, CA) filled with 2ml of 50 mM borate buffer and 100 μ L of reaction mixture, 200 μ L of an acetone solution of fluorescamine was added. The reaction mixture was shaken vigorously for about 2 minutes and then diluted to 4 mL with deionized, double distilled water. CE measurements were carried out within 10 minutes after the derivatization. The derivatization reaction is showed in Figure 14

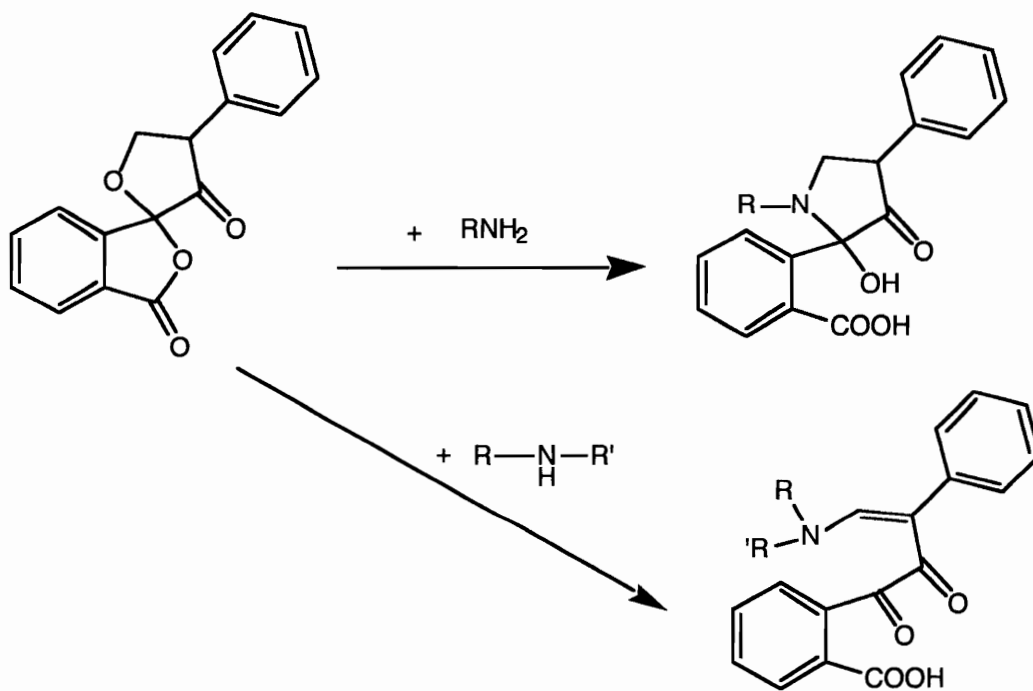


Figure 14. Reactions of fluorescamine with primary and secondary amines.

2.3. CZE Analysis of Ranitidine in Urine Sample

2.3.1. Instrumentation

This part of the work was carried out on a Beckman P/ACE System 2100 instrument (Beckman, Fullerton, CA) described previously.

2.3.2. Chemicals and Materials

Ranitidine from Sigma Chemical Co. (St. Louis, MO) was used for the analytical standard and for spiking. Phosphoric acid and sodium phosphate were purchased from Aldrich Chemical Company (Milwaukee, WI).

A solid phase extraction cartridge, SPEC®-PLUS™-3ML-C18AR with filter, was purchased from Ansys. Inc (Irvine, CA). A 'Baker'-10™ extract system with a pressure gauge was from J.T. Baker Inc. (Phillipsburg, NJ). A water aspirator was used for creating vacuum.

2.3.3. Sample Preparation

The stock ranitidine (1000 ppm) solution was prepared by dissolving 0.25 gram in 250 mL deionized, double distilled water. Other solutions were prepared from this stock solution.

Solid phase extraction was performed as follows: 1) column conditioning was carried out by aspirating 0.5 ml of methanol and 0.5 mL of phosphate buffer through the column with a gentle vacuum (2 inches of Hg) without allowing the

column to dry; 2) sample addition and washing was carried out by applying 1 mL of sample to the column, aspirating then washing with 1 mL of deionized water; 3) the column was air dried for three minutes; 4) sample elution was carried out by applying 2 x 0.5 mL methanol and aspirating through the column. The elute was collected and the methanol was removed by rotary vaporization. After removal of the methanol, one mL of phosphate buffer was added and the solution was ready for CZE measurements. Figure 15 shows the extraction sequence.

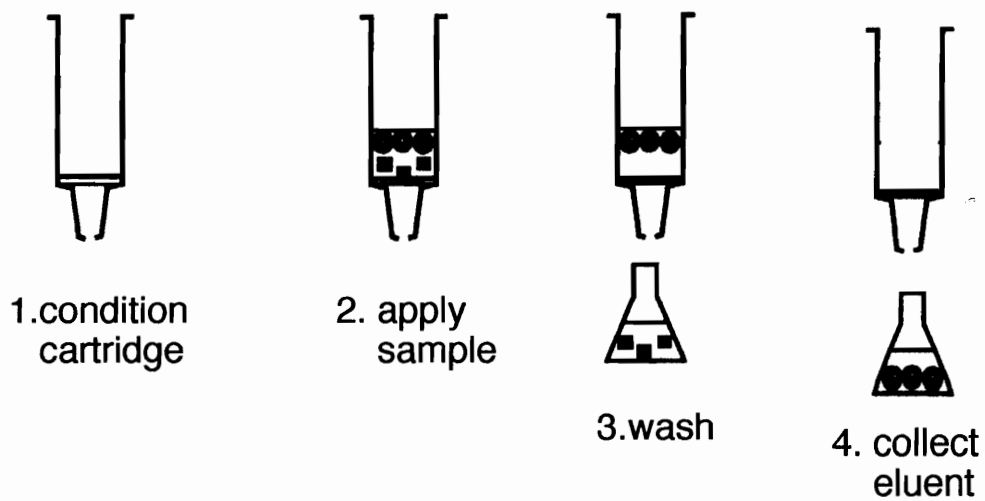


Figure 15. Extraction sequences in SPE. Four steps to perform SPE experiment.

2.4. Non Aqueous CE

2.4.1. Instrumentation and Chemicals

The instrument used in this work was a Beckmen P/ACE 2100, which was described previously.

N-methylformamide (NMF), dimethylsulfoxide (DMSO), toluene, dinitrobenzoic acid, terephthalic acids, hemellitic acid and trimellitic acid were purchased from Sigma Chemical Company (St. Louis, MO). All the chemicals were used as purchased.

2.4.2. Sample Preparation

A 200 ppm solution of each chemical was prepared by dissolving 2 mg of compound in 10 ml N-methylformamide solvent.

CHAPTER III. RESULTS AND DISCUSSIONS

3.1. CZE for Polyimide Analyses

3.1.1. Properties of Polyimides

A polyimide was first produced in 1908 by Bogert and Renshaw ⁽⁸⁷⁾ by the thermal dehydration of 4-aminophthalic anhydride. Over the past several decades, polyimides have become an increasingly important class of polymers. Their excellent thermal and mechanical properties make them well suited for many high performance applications in the aerospace and microelectronics industries, including uses as composite matrix resins, moldings, coatings, adhesives and for electronic packaging.

As the requirements for many special applications, particularly in the microelectronics and aerospace industries, have become sophisticated, there has been a need to improve the properties of conventional polyimides. Needed are polyimides with high glass transition temperatures, good long term thermal stability, lower dielectric constant, lower water absorption and better processability. To achieve these goals, different kinds of monomers and end cap groups are synthesized and used to make polyimides.

Under normal conditions, polyimides are very stable (up to 360°C). But at high temperature and in the presence of concentrated bases or acids, polyimides will undergo hydrolysis to form aromatic diamines and aromatic tetracarboxylic acids or salts. CZE will show unique advantages to separate

these small and non-volatile decomposition products. The fusion reaction of a polyimide is showed in Figure 16.

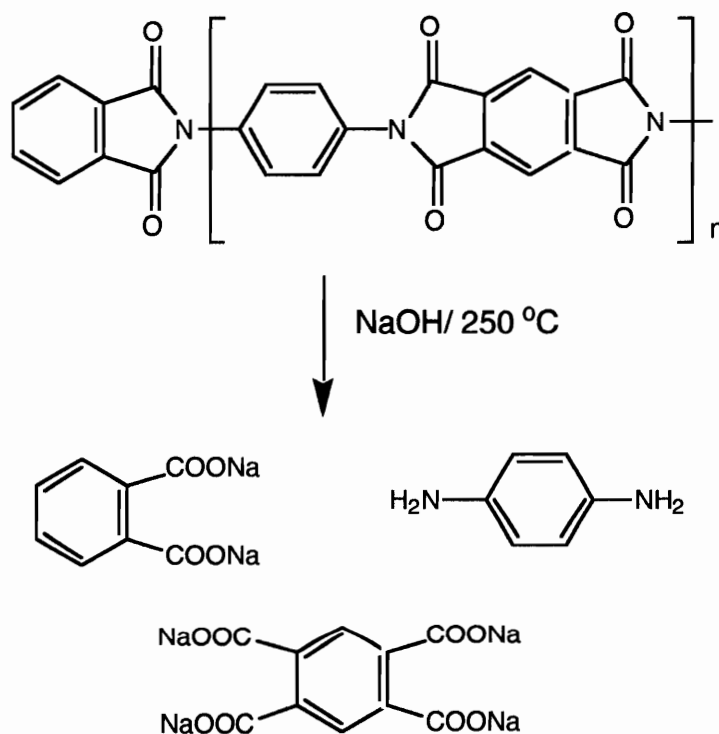


Figure 16 Fusion reaction of a polyimide.

3.1.2. BTDA-pPDA-PA Analysis

This polyimide was synthesized from the dianhydride BTDA, and 1,4-phenylenediamine (pPDA). The end capping group was from phthalic anhydride (PA). Their structures are shown in Figure 17

Two different buffer solutions (75 mM sodium borate (pH 9.2) and 25 mM sodium phosphate (pH 8.2)) were used in this part of the work.

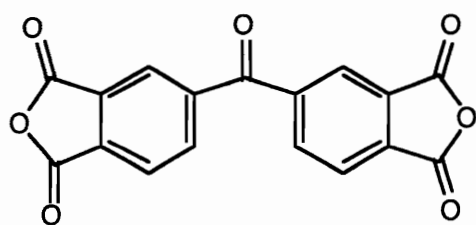
Figure 18 shows the electropherogram of a sample with two added compounds, phthalic acid and terephthalic acid, using 75 mM sodium borate buffer solution (pH 9.2). Phthalic acid and terephthalic acid were added to demonstrate the separation capability of CE. Four main peaks are shown: Peak 1 is an aromatic diamine, which is a neutral molecule and therefore carried through the column by electroosmotic flow. Peaks 2 and 3 are the phthalate and the terephthalate anions respectively. They were well separated by CE in borate buffer solutions. Peak 4 is from the BTDA. It has four negative charges at this pH condition so it elutes much later due to its high electrophoretic mobility.

Figure 19 shows the electropherogram of a polyimide sample in 75 mM borate buffer solution (pH=9.2). Peak 1 is the aromatic diamine, peak 2 is the phthalate anion and peak 3 is from the BTDA. Phthalic anhydride was added in the making of the polyimide in order to act both as a end-capping group and as a reagent to adjust the polymer molecular weight.

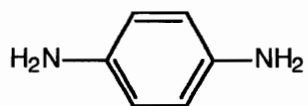
Figure 20 shows an electropherogram of the same polyimide sample solution in 25 mM Na₂HPO₄ buffer solution (pH=8.2). Here there are three well separated peaks which elute early: peak 1 is the aromatic diamine, peak 2 is

the phthalate anion and peak 3 is from the BTDA. There are differences in migration times between the two buffer solutions, especially for anions. This can be explained by the fact that the borate buffer solution is higher in pH than the phosphate buffer, so the polycarboxylic acid bears more negative charge with a resultant higher electrophoretic mobility.

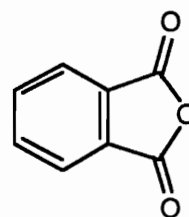
In the phosphate buffer solution the phthalate anion cannot be separated from the terephthalate anion. Figure 21 shows the electropherogram of a mixture of phthalate and terephthalate acids. Peak 2 represents the coelution of both phthalate and terephthalate anions.



BTDA



pPDA



PA

Figure 17. Structures of monomers for the polyimide of BTDA-pPDA-PA

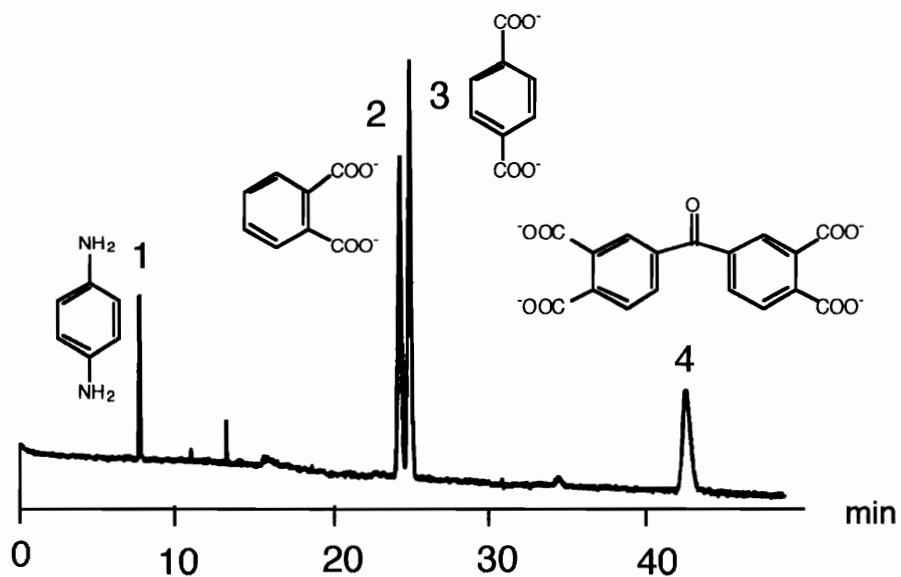


Figure 18. Electropherogram of polyimide sample mixture containing phthalic and terephthalic acids. Buffer: 75 mM borate, pH 9.2; voltage 10.0 kV (current: 40 μ A); temperature 25°C; detection: UV, 254 nm; column: 61 cm x 75 μ m (I.D.) with 47 cm to detector. Peak 1 is the aromatic diamine, peak 2 phthalate anion, 3 terephthalate anion and 4 BTDA anion.

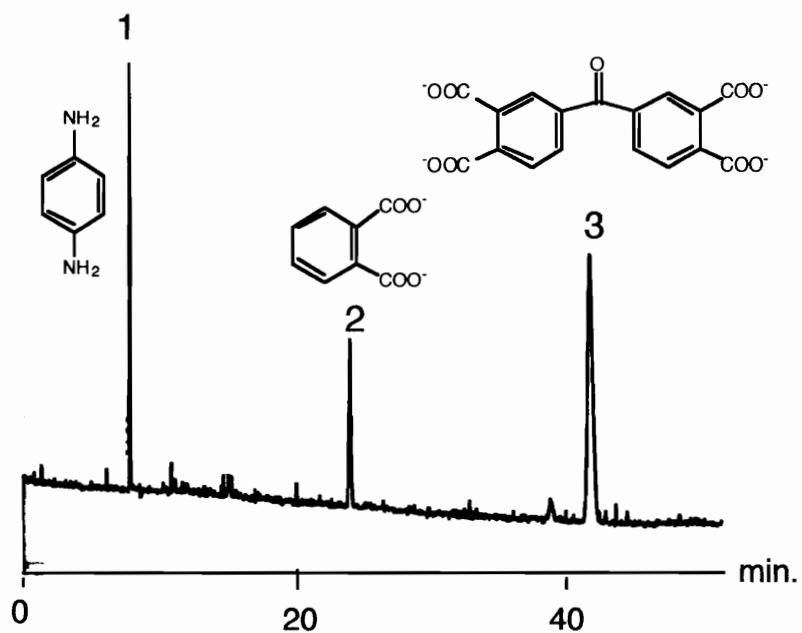


Figure 19 Electropherogram of polyimide sample. Buffer: 75 mM borate, pH 9.2; voltage 10.0 kV (current: 40 μ A); temperature 25°C; detection: UV, 254 nm; column: 61 cm x 75 μ m (I.D.) with 47 cm to detector. Peak 1 is the aromatic diamine, peak 2 phthalate anion, peak 3 DBTA anion.

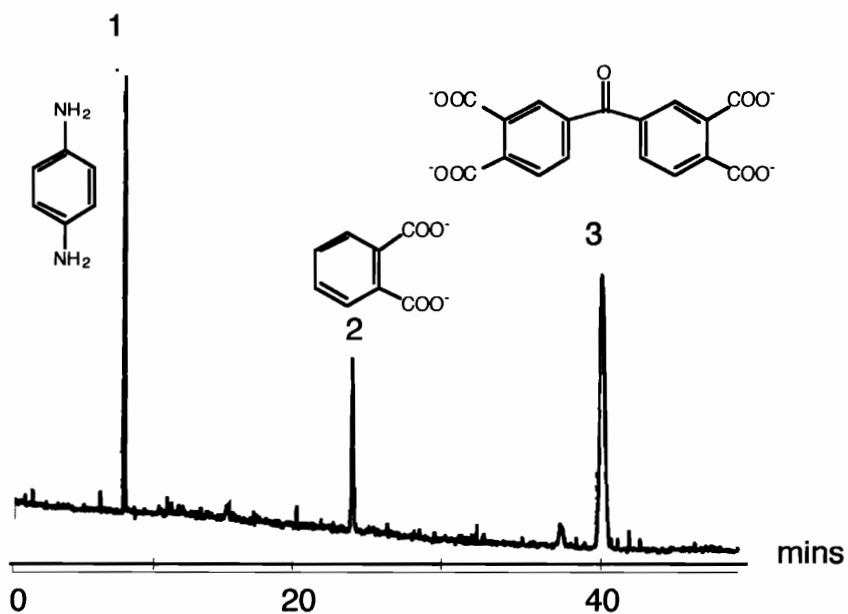


Figure 20. Electropherogram of sample in 25 mM Na₂ PO₄ buffer solution (pH=8.2). Voltage:10 kV, current: 25 μA), pH 9.2; temperature 25°C; detection: UV, 254 nm; column: 61 cm x 75 μm (I.D.) with 47 cm to detector. Peak 1 is aromatic diamine, peak 2 phthalate anion and peak 3 DBTA anion.

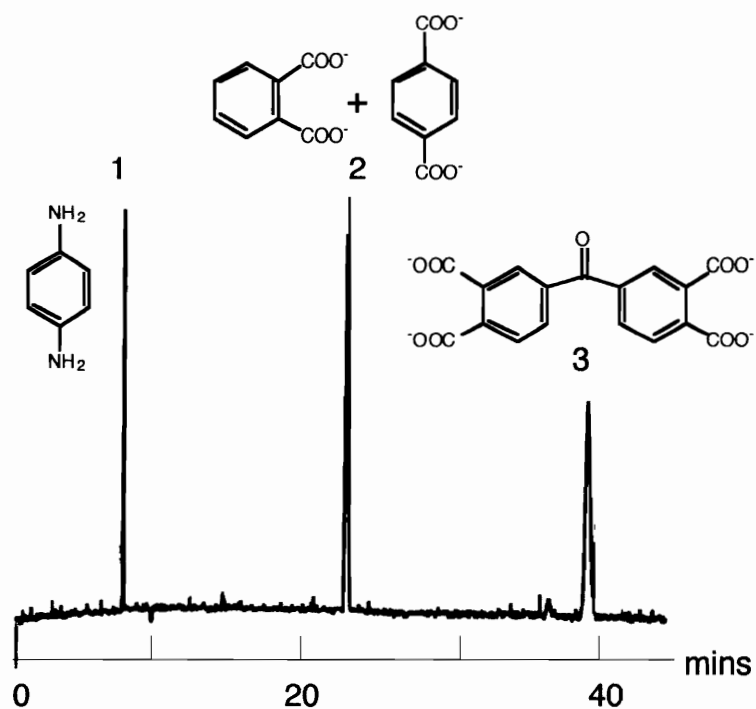


Figure 21. Electropherogram of mixture of polyimide sample with phthalic and terephthalic acid in 25 mM Na_2PO_4 buffer solution (pH = 8.2): voltage:10 kV, current: 25 μA ; pH 9.2; temperature 25°C; detection: UV, 254nm; column: 61 cm x 75 μm (I.D.) with 47 cm to detector. Peak 1 is aromatic diamine, peak 2 phthalate anion and terephthalate anion and peak 3 DBTA anion.

3.1.3. BAPB-BPDA-PA Analysis

This polyimide was synthesized from the 3,4,3',4'-biphenyltetracarboxylic dianhydride (BPDA), and BAPB, with the end-capping group, PA. The structures of these compounds are shown in Figure 22. The purpose of using BAPB as monomer is that it contains an aromatic ether linkage in the molecule, which introduces a flexible spacer in the final polyimide product. Processability of polyimides has been greatly enhanced by incorporating flexible spacers⁽⁸⁸⁾. It also has been shown that the influence of the diamine structure on the stability of polyimide is significant⁽⁸⁹⁾.

The electropherogram of the decomposition products is shown in Figure 23. It does not show a large peak for the diamine, BAPB, which should appear early because the diamine is neutral in the basic borate buffer solution. This situation can be explained by the fact that BAPB is a very hydrophobic compound and has a limited solubility in the inorganic borate buffer solution. Three small peaks (peaks 1, 2 and 3) are the decomposition products of BAPB, which is not so stable at high temperature, and is suspected to be decomposed by sodium hydroxide at high temperature. The structures of these peaks remain unknown due to the limitations of the UV detector. Peak 4 is the end-cap group, PA, which carries two negative charges. Peak 5 is the monomer BPDA, which is very stable and carries four negative charges.

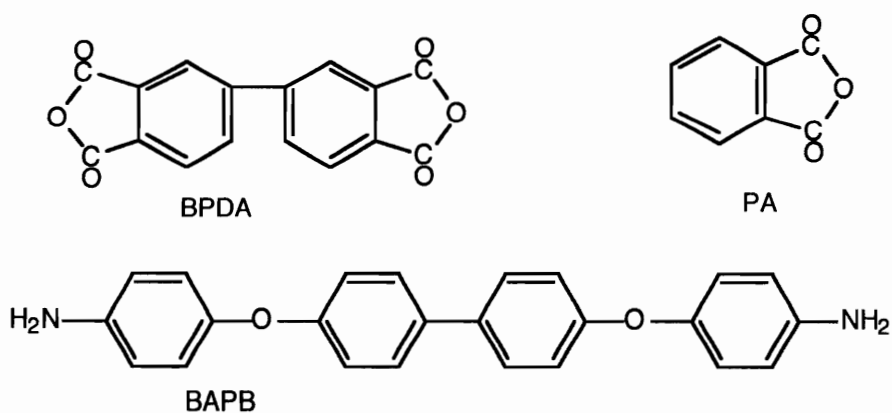


Figure 22. The structure of BAPB, BPDA and PA

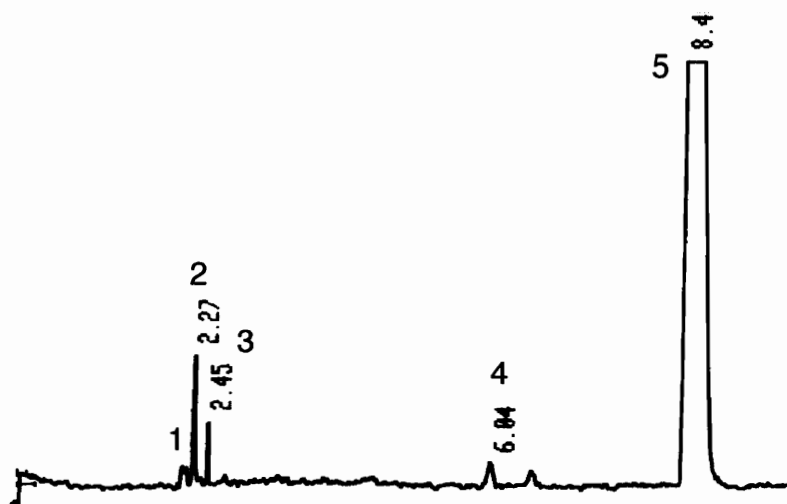


Figure 23. Electropherogram of decomposed products from BAPB-BPDA-PA polyimide. Experimental conditions: 50 mM borate buffer (pH = 9.2). column: 75 μm x 37 cm (Ld = 25 cm). Voltage: 10 kV. UV 254 nm.

3.1.4 PMDA-DAPPO Analysis

This polyimide was synthesized from pyromellitic dianhydride (PMPA), and bis(4-aminophenyl) phenyl phosphine oxide (DAPPO). Their structures are shown in Figure 24. There was no end-cap group present in this product. The DAPPO was used as a monomer because it contains a phosphorus atom. Phosphorus is widely used in synthetic polymers due to its fire retardant property.

The electropherogram of the decomposition products from this polyimide is shown in Figure 25. There are two early peaks: peak 1 is the diamine DAPPO and peak 2 is the decomposition product of DAPPO. The dynamic TGA thermogram of PMPA-DAPPO shows that the polyimide loses 5% of its total weight when temperature reaches 100°C; then the polyimide was stable up to 550°C (90). The 5% weight loss is probably water. The structure of the compound of peak 2 remains unknown. Peak 3 is PMPA, which is small in size and carries four negative charges.

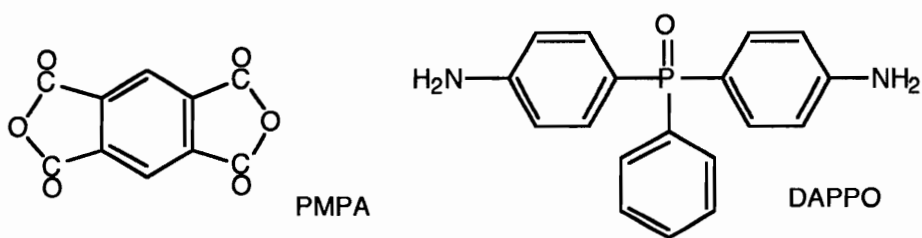


Figure 24. Structures of PMPA and DAPPO



Figure 25. Electropherogram of the decomposition products from PMPA-DAPPO polyimide. Experimental conditions: 50 mM borate buffer (pH = 9.2). column: 75 μ m x 37 cm (Ld = 25 cm). Voltage: 10 kV. UV 254 nm. Peak 1 and 2 are from DAPPO, and 3 is PMPA ion.

3.1.5. 6FDA-DAPPO Analysis

This polyimide was synthesized from 5,5'-[2,2,2-trifluoro-1-(trifluoromethyl)ethylene] bis-1,3-isobenzofurandione (6FDA), and the diamine DAPPO. Their structures are shown in Figure 26. There is no end-cap group present in this polyimide. As discussed previously, DAPPO is used in the synthesis of polymers for fire retarded applications. It has been demonstrated that fluorine containing polyimides show improved processability ⁽⁹¹⁾, low dielectric constant and low water absorption while maintaining excellent thermal stability. They have found applications as composite matrix resins ⁽⁹¹⁾, as interlayer dielectrics used in microelectronics ⁽⁹²⁾ and as gas separation membranes ⁽⁹³⁾. So 6FDA was used as a monomer to synthesize this polyimide.

The electropherogram of the decomposition products from this polyimide is shown in Figure 27. Again, there are two peaks that elute early. Peak 1 is DAPPO and peak 2 is the decomposition product from DAPPO but the structure is unknown. They are the same pattern as in the polyimide of PMDA-DAPPO. There are other peaks that elute late. Peak 4 is 6FDA and peak 3 and 5 are the decomposition products from 6FDA. The detailed structures of peaks 3 and 5 and the detailed decomposition reaction of 6FDA are unknown.

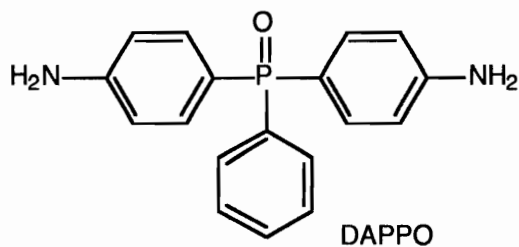
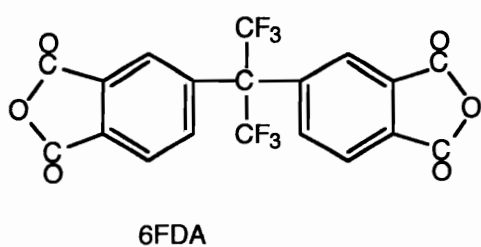


Figure 26. Structures of 6FDA and DAPPO

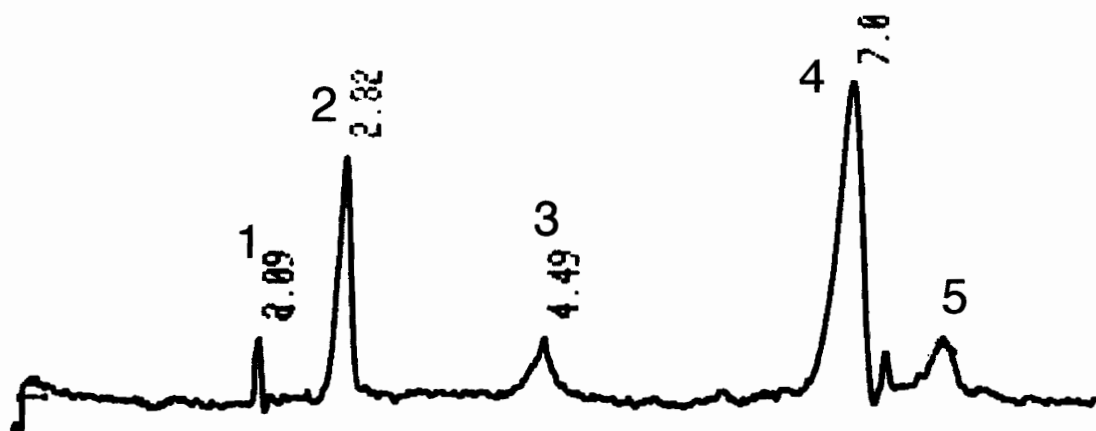


Figure 27. Electropherogram of the decomposed products from 6FDA-DAPPO polyimide.. Experimental conditions: 50 mM borate buffer (pH = 9.2). column: 75 μ m x 37 cm (Ld = 25 cm). Voltage: 10 kV. UV 254 nm.

3.1.6. BisA-DA-pPDA, mPDA-4-PEPA Analysis

This polyimide was synthesized from bisphenol A bis(phthalic dianhydride) (BisADA), pPDA (70 %) and mPDA (30 %). It also had an end capping group, 4-(phenylethyl) phthalic dianhydride (4-PEPA). Their structure are shown in Figure 28. The BisADA contains aromatic ether groups that introduce flexibility into the polyimide and enhance the processability of the product. 4-PEPA is a specially designed end cap group; it contains an unsaturated bond that can be cured after the polyimide is synthesized. It has been demonstrated that curing the polyimide greatly increases the thermal stability and other properties (98). It is interesting to note what structural changes occur before and after curing of this polyimide. Other analytical methods such as NMR and IR were tried in this study, but no peaks could be identified(98).

Before curing, the polyimide decomposed at 240°C. The electropherogram of the decomposition products is shown in Figure 29. It is very difficult to assign peaks to corresponding monomers and end capping group. After spiking with the end capping group, the electropherogram is shown in Figure 30. Peak A is the end capping group. After spiking this mixture again with the BisADA and end capping group, the electropherogram is shown in Figure 31. Peak B is the BisADA. Comparing these three electropherograms, we can see that both the end capping group and the BisADA were decomposed in the process of fusion reaction of this polyimide. Again, these decomposition products remain unknown.

The difference between the polyimide before and after curing is shown in Figure 32 and 33. The polyimides were decomposed under identical conditions. The differences between them are obvious. The polyimide before curing gives more peaks later in the electropherogram. The polyimide after curing gives a smaller number of products after decomposition. Unfortunately, no means was available to determine the structure of the decomposition products from this experiment.

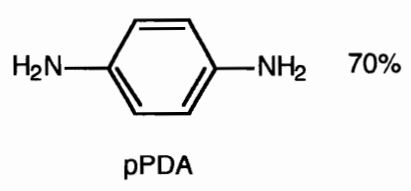
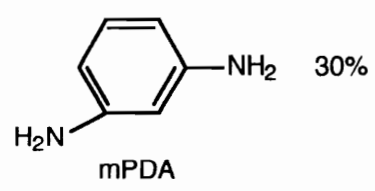
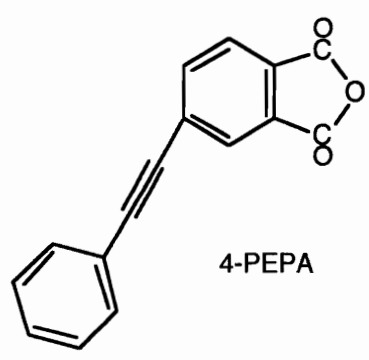
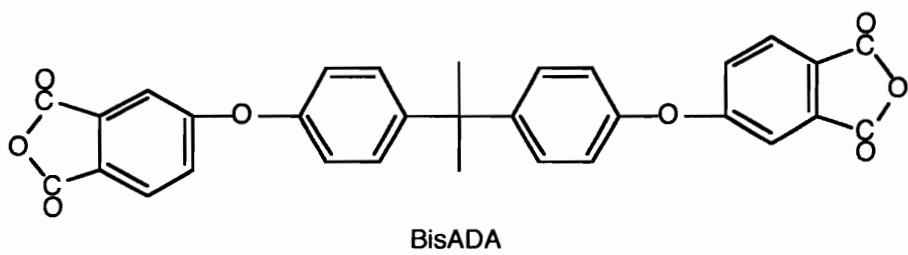


Figure 28. Structures of monomers and end cap compounds for polyimide BisADA-pPDA, mPDA-4-PEPA

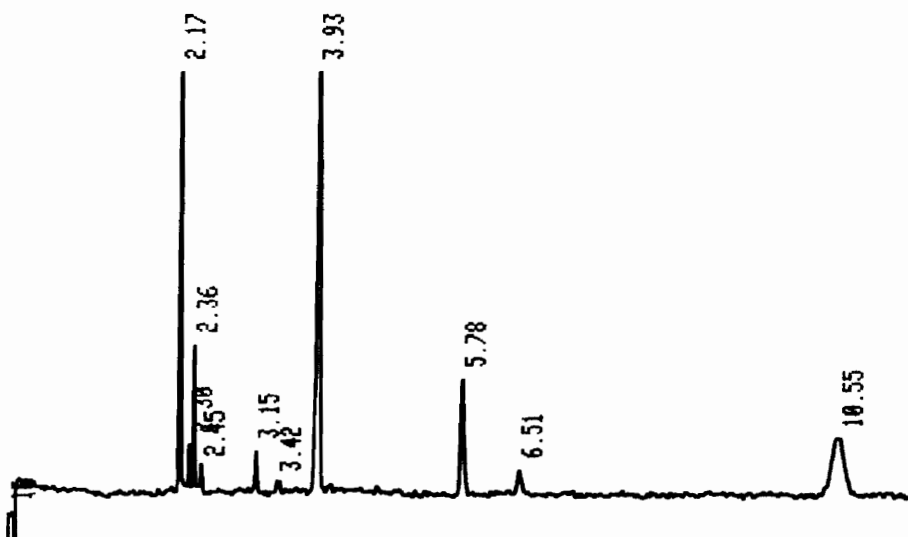


Figure 29. Electropherogram of decomposed products from BisA-DA-pPDA. Experimental conditions: 50 mM borate buffer (pH=9.2). Column: 75 μm x 37 cm (Ld = 25 cm). Voltage: 10 kV. UV 254 nm.

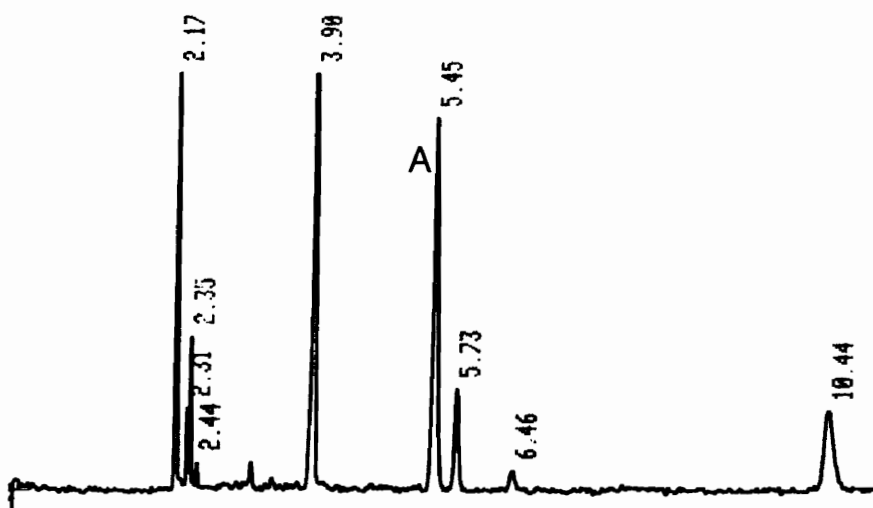


Figure 30. Sample in Figure 29 spiked with end cap group. Conditions are the same as Figure 29.

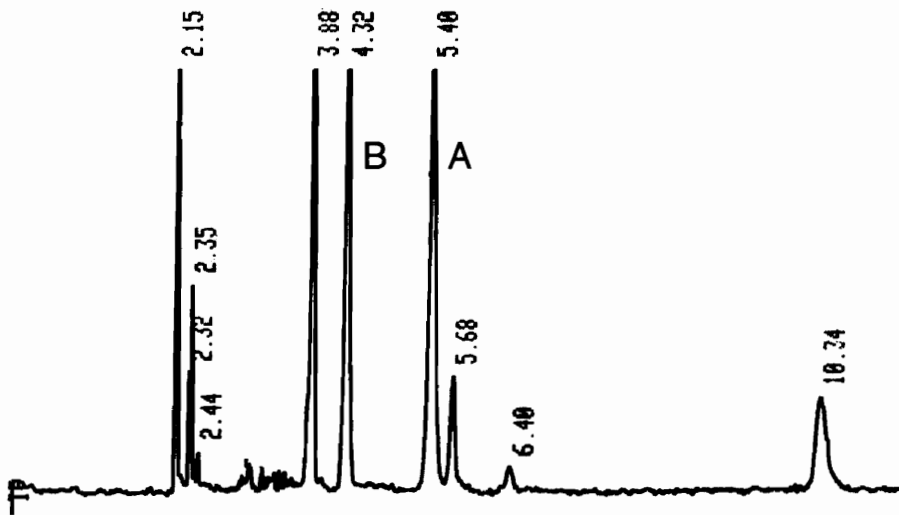


Figure 31. Electropherogram of mixture in Figure 29 spiked with BisADA and end cap group. Condition are the same as Figure 29. Peak A is end cap group and peak B is BisADA.

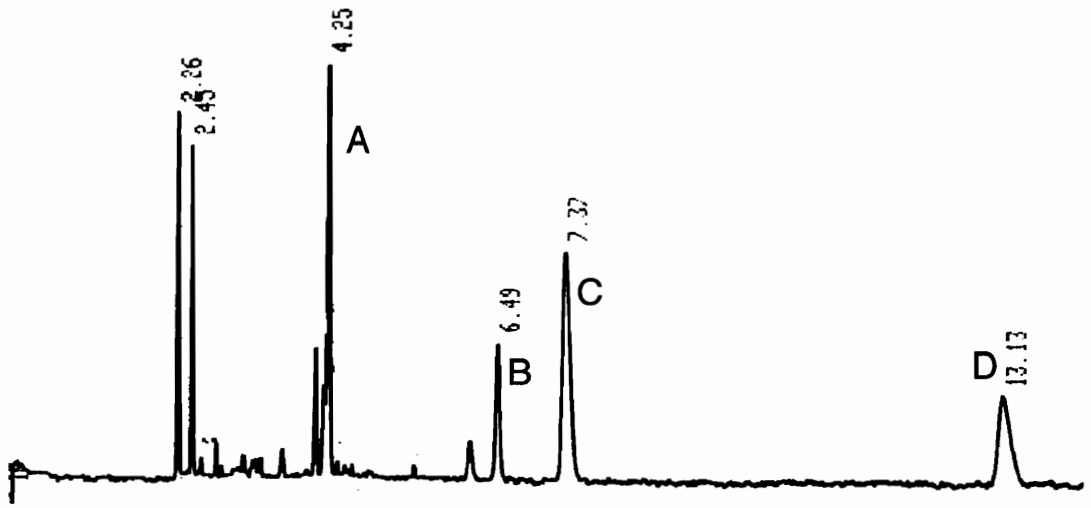


Figure 32. Electropherogram of decomposition products of polyimide before curing

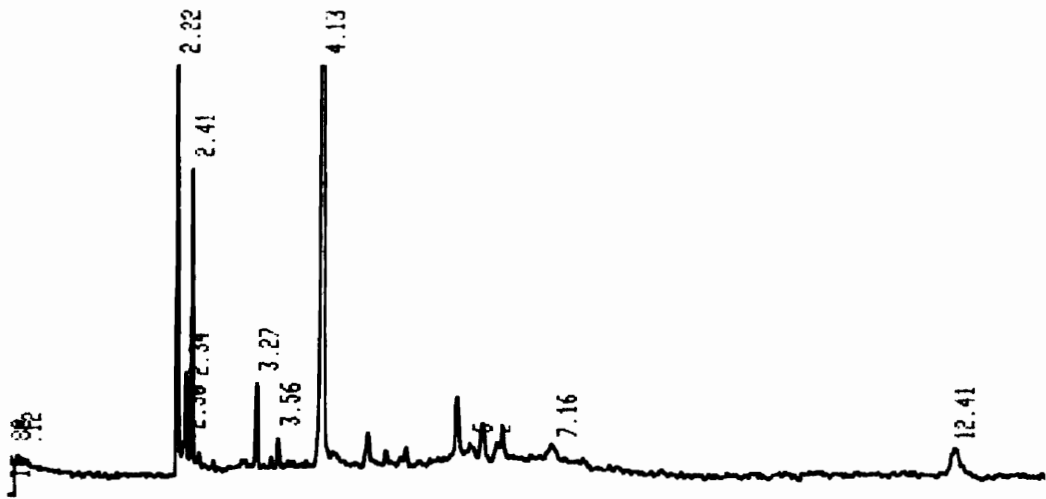


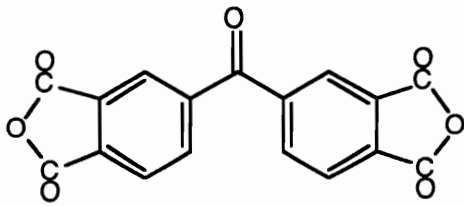
Figure 33. Electropherogram of decomposition products of polyimide after curing.

3.1.7. BTDA-DAPPO Analysis

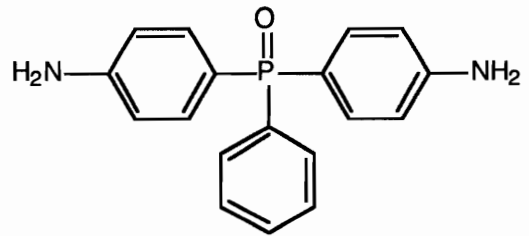
This polyimide was synthesized from BTDA and diamine DAPPO. The structure of monomers is shown in Figure 34. There is no end capping group in this polymer.

From the electropherograms of previous polyimides, it can be seen that there are two early peaks produced from DAPPO. Is it just a coincidence or is it a unique decomposition way of DAPPO at high temperature? It is an important question to study.

The electropherogram of this polymer is shown in Figure 35. Once again, two peaks elute early. They show the same pattern as in previous polymers which contain DAPPO monomer. Peak 4 is BTDA and peak 3 is the phthalate ion. Since there is no end capping group presence in this polymer, peak 3 must be the decomposition product from BTDA. BTDA is also the monomer in first polyimide investigated, in which an end capping group is present. From Figure 20, it can be seen that peak 2 (phthalate ion) is large. This means that the amount of phthalate ion is more than that of end capping group. This could mean that some phthalate ion comes from the decomposition of BTDA.



BTDA



DAPPO

Figure 34. Structures of BTDA and DAPPO

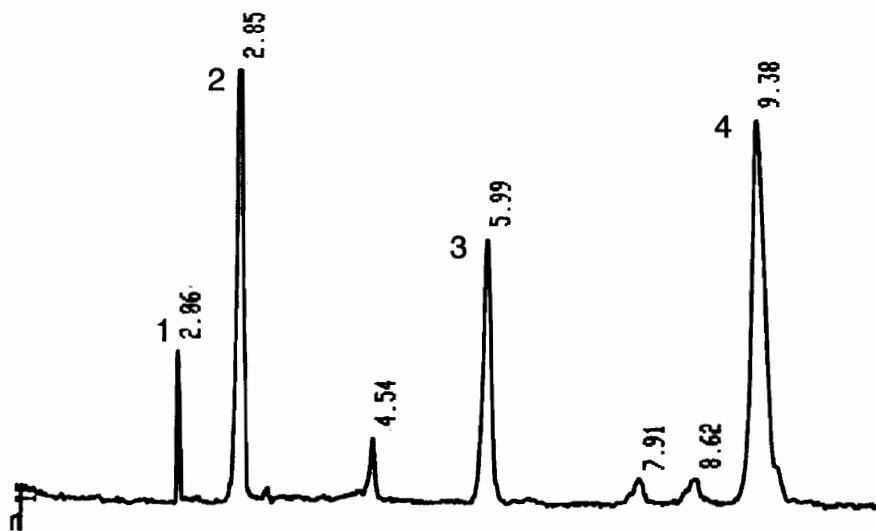


Figure 35. Electropherogram of polyimide BTDA-DAPPO. Experimental conditions: 50 mM borate buffer (pH = 9.2). column: 75 μ m x 37 cm (Ld =25 cm). Voltage: 10 kV. UV 254 nm.

3.1.8. Conclusions for Polyimides Analysis

There are more than ten electropherograms from polyimides presented in this research. If the polyimide is made from stable, and simple monomers such as pPDA, PMPA and BPDA, the electropherogram is simple. It is easy to assign elution peaks to their corresponding monomers. Otherwise, complicated electropherograms can be obtained. This situation is caused by the decomposition of monomers at high temperature. One example is the polyimide BisA-DA-pPDA, and mPDA-4-PEPA, the electropherogram of this polyimide is too complicated to identify peaks, because both the monomer and the end capping group are decomposed at high temperature.

In the early days of pyrolysis GC analyses of polymers, where on-line MS was not available, the decomposition products were complex and it was impossible to identify the structures for many peaks. This did not prevent the application of this technique for polymer analyses. The reason is that polymers demonstrated different patterns in their pyrolysis chromatograms due to the difference in monomers. However, the same pattern could be obtained if the same monomer were used to synthesize the polymer.

In the analysis of polymer by CZE, the polyimide is decomposed by base at high temperature. The amounts of reagents, temperature and time for the decomposition reaction can be accurately controlled. It is reasonable to get the same (or similar) decomposition products from the same reactants.

It is not difficult to see that: (1) different polyimides show different patterns in electropherograms; this means the decomposition products from different polyimides are different; (2) the same monomer shows similar pattern in

electropherogram even from different polyimides, this implies that the same monomer will produce similar products after decomposition reaction; and (3) the pattern of an electropherogram can be considered as a “finger print” of the polyimide, and that can be used for major composition determination, as in pyrolysis GC analysis.

Compared to pyrolysis GC, this method produces smaller numbers of decomposition products due to the mild decomposition conditions. The structures of these products are also close to the original structures of the monomers. If a CE-MS instrument was available, it would be possible to make the complete compositional analysis for polyimides.

3.2. CZE FOR NYLON ANALYSES

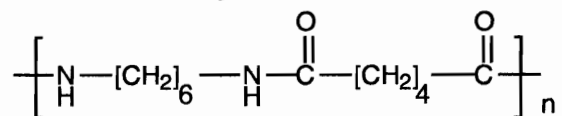
3.2.1 Properties of Nylons

Nylon-6/6 was developed by Carothers in the 1930's and became the first and most widely used engineering plastic ⁽⁹⁵⁾. Nylon 6/6 is a condensation polymer of a 6 carbon dicarboxylic acid (adipic acid) and a 6 carbon diamine (hexamethylenediamine). The amide groups (-CONH-) provide stiffening to the polymer and the methylene groups (-CH₂-) between the amide groups provide flexibility to the polymer. Nylon 6/9 is a condensation polymer of nonanedioic acid (9-carbon acid) and hexamethylenediamine (6 carbons).

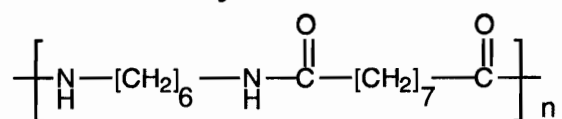
Nylons are characterized by high impact resistance, good abrasion resistance, and resistance to many corrosive solvent. Injection molded nylon is used for gears and other automobile components. High impact, amorphous nylon is used for power tool housings and radiator fans.

According to the chemical structure, there are three types of nylons. The first is the condensation product of a dicarboxylic acid and a diamine. After hydrolysis, both the original dicarboxylic acid and the diamine are formed. The second type is the product of a ring opening reaction or condensation reaction of ω -aminocarboxylic acid. After decomposition, only one product, ω -amino carboxylic acid is formed. The third is the copolymer of types one and two. Figure 36 shows the nylons studied in this work.

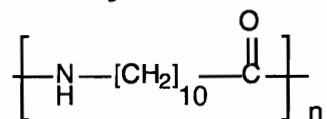
nylon 6/6



nylon 6/9



nylon 11



nylon 12

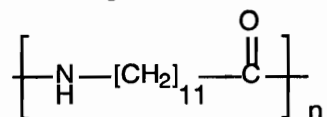


Figure 36. Structures of nylons studied in this work.

3.2 2. The Decomposition of Nylon by Acid

Under either acidic or basic conditions nylons will be hydrolyzed to the starting carboxylic acid and amine. For basic hydrolysis, sodium hydroxide is most often used ⁰. For acidic hydrolysis, sulfuric, phosphoric, hydrochloric and hydrobromic acid are all used . In this work, hydrobromic acid was used because it is volatile and has a relatively high boiling point. The high boiling point is beneficial to the hydrolysis reaction because high temperatures can be used in the decomposition reaction. Volatility is a must for the easy removal of the excess hydrobromic acid after reaction. Although phosphoric acid is also a good acid for hydrolysis of nylons, it is necessary to add large amounts of sodium hydroxide after the reaction to neutralize the excess acid. This results in a high salt concentration and produces peak broadening in CE analysis ⁽⁹⁶⁾. The decomposition reaction of nylon in acidic conditions is shown in Figure 37

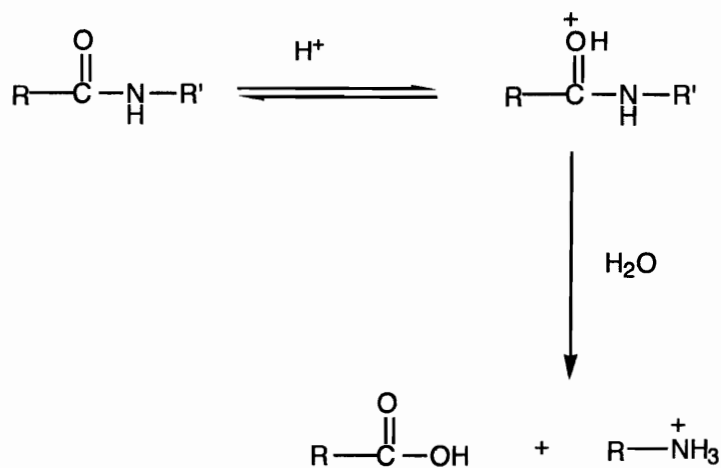


Figure 37. Amide (nylons) decomposition in acidic solution.

3.2.3 The Analysis of Nylon 6/6 and 6/9

The decomposition of nylon 6/6 and nylon 6/9 produces the two corresponding monomers: diamines and dicarboxylic acids. For complete compositional analysis, it is necessary to analyze both the diamine and the dicarboxylic acid.

There are three separation techniques which are used for amine analyses: Gas Chromatography (GC), High Performance Liquid Chromatography (HPLC) and Capillary Electrophoresis (CE).

For GC, derivatization is necessary to perform amine analysis. Primary amines are very basic and very polar. They are adsorbed by acidic spots in the GC column and often cause tailing problems, sometime even complete adsorption has occurred. Usually silylation reagents ⁽⁹⁷⁾ and acylation reagents ⁽⁹⁸⁾ are used to produce stable and volatile derivatives for GC analysis. These derivatizations however are both time consuming and tedious. Another problem is created by the derivatization of polyamines. Several active hydrogen atoms must be derivatized by the reagent. But all of the derivatization reactions are not 100 percent complete due to steric hindrance of the N-substituted group ⁽⁹⁹⁾. Thus, several products may be obtained from a single polyamine "molecule", causing severe problems when trace amine analysis is performed. Recently, there is an amine GC column ⁽¹⁰⁰⁾ commercially available, which makes it possible to do amine analyses without any derivatization. However, this column is limited to low boiling point amines, usually monoamines .

For HPLC and CE analysis of amines, derivatization is also necessary. First, amines show very weak UV absorption and it is difficult to detect them by a conventional UV detector. Secondly, they are very basic and will be adsorbed by acidic sites in the HPLC column. The derivatization of amines with fluorescent moieties or UV moieties has been well developed for HPLC (101-103).

The analyses of amino acids by CE is well documented in the literature(104-107). The most used derivatization reagents are dansyl chloride (108), fluorescein isothiocyanate (FITC) (109), fluorescamine (110), 9-fluorenylmethyl chloroformate (FMOC) (111) and o-phthalaldehyde (OPA) (112). Fluorescence detectors are often used to provide both selectivity and high sensitivity. Most fluorescence derivatives also can be detected by UV detector as well.

Fluorescamine (4-phenylspiro[furan-2(3H),1'phthalan]-3,3'-dione) was chosen for this work. This reagent reacts readily at alkaline pH with both primary and secondary amines (112). The excess reagent is quickly hydrolyzed in aqueous solution, while the derivative it forms is not. At pH 9 and room temperature, the reaction between fluorescamine and primary amines has a half-time of 200-1000 ms, while the hydrolytic decomposition of the reagent has a half-time of several seconds (113). So, upon mixing fluorescamine with a basic aqueous amine solution, there is immediate derivatization followed by rapid hydrolysis of unreacted reagent. The reaction scheme of fluorescamine with primary and secondary amines is shown in Figure 14. This reagent not only adds a UV moiety to the amine, it also introduces a negative charge that the derivative can both be separated by CZE and detected by UV. Other

derivatization reagents such as dansyl chloride and Fmoc introduce a UV moiety to the derivative as well but not a negative charge. That means that micellar electrokinetic capillary chromatography (MECC) must be used to separate these derivatives.

The derivatives of diamine and fluorescamine can be easily separated and detected by CZE with an on-line UV detector. Figure 38 shows the electropherogram of a solution containing only borate buffer and fluorescamine. Peak 1 is acetone and peak 2 is the hydrolytic product from fluorescamine. Figure 39 is the electropherogram of nylon 6/6 derivatized with fluorescamine. Peak 1 is acetone, peak 2 appears on the shoulder of the acetone peak. This molecule must have a small charge to size ratio, and it may indicate the presence of oligomers formed from the decomposition of nylon. From the decomposition mechanism, we can see that the decomposition is an equilibrium reaction. Peak 3 is hexamethylenediamine. After derivatization with fluorescamine it bears two negative charges in the borate buffer solution and elutes later. Peak 4 is unknown; it may be an impurity in the product. We have been unsuccessful in collecting sufficient amount of peak 4 for MS analysis. Peak 5 is the hydrolytic product of fluorescamine. The electropherogram of nylon 6/9 derivatized with fluorescamine is the same as that of nylon 6/6, because they are made from the same diamine.

Aliphatic acid analyses can also be performed by GC, HPLC or CE. For GC analysis, derivatization is still necessary. Aliphatic acids are usually non-volatile and polar compounds. The derivatization is usually carried out by esterification with an alkyl group⁽¹¹⁴⁾ or silylation⁽¹¹⁵⁻¹¹⁶⁾. The derivatives are

volatile compounds and suitable for GC analysis. The major limitation is that tedious purification is necessary before derivatization for many samples.

For HPLC analysis, aliphatic acids are usually converted to their UV-VIS absorbing esters by reaction with aromatic halides such as phenacyl bromide (117), or naphthacyl bromide (118). These derivatizations should be performed in an aprotic solvent such as DMSO (119,120). The separation of acids from diamines is necessary before the derivatization steps.

For CZE analysis, diacids can be easily separated in a borate buffer solutions, but they are difficult to detect. Usually they are detected by indirect UV (121), conductometric detection (122) or by direct UV detection at low wavelength (123). In this work, direct UV at a wavelength of 200 nm was employed. Figure 40 shows the separation of a mixture of decomposition products from nylon 6/6 and nylon 6/9. Peak 1 is diamine. It elutes in the dead time (t_0) and is broader and larger compared to other peaks. This can be explained by the facts: 1) amine has stronger UV absorption at 200 nm than carboxylic acids do, and 2) hexamethylenediamine is neutral in borate buffer solution (pH=9.2), so it elutes at t_0 . There are probably small amounts of oligomers present in the mixture due to the incomplete decomposition of nylon. They are large and the ratio of charge to size is close to zero. They also elute close to t_0 . Peak 2 is the nonanedioic anion and peak 3 is an adipic anion. They were well separated by CZE in this borate buffer solution.

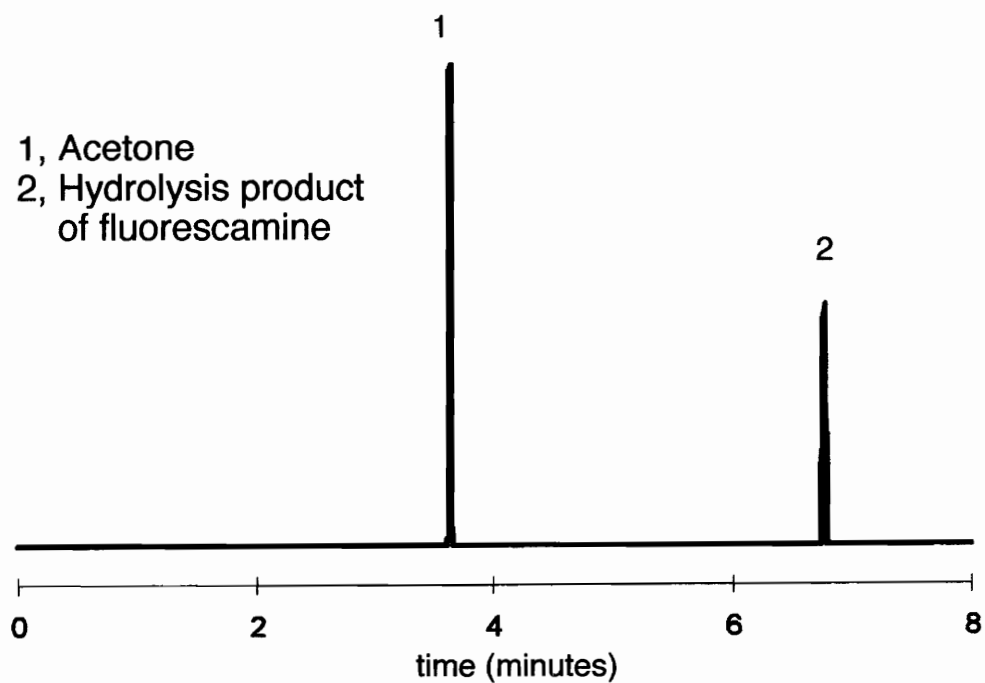


Figure 38. Electropherogram of fluorescamine in borate buffer solution.
Condition: 75 mm x 57 cm capillary ($L_d = 50$ cm); +15 kV applied
Voltage; 50 mM borate buffer, pH = 9.2; temperature 25 °C;
injection: 3 psi for 2 seconds; wavelength = 280 nm. Beckman P/ACE
2100 instrument.

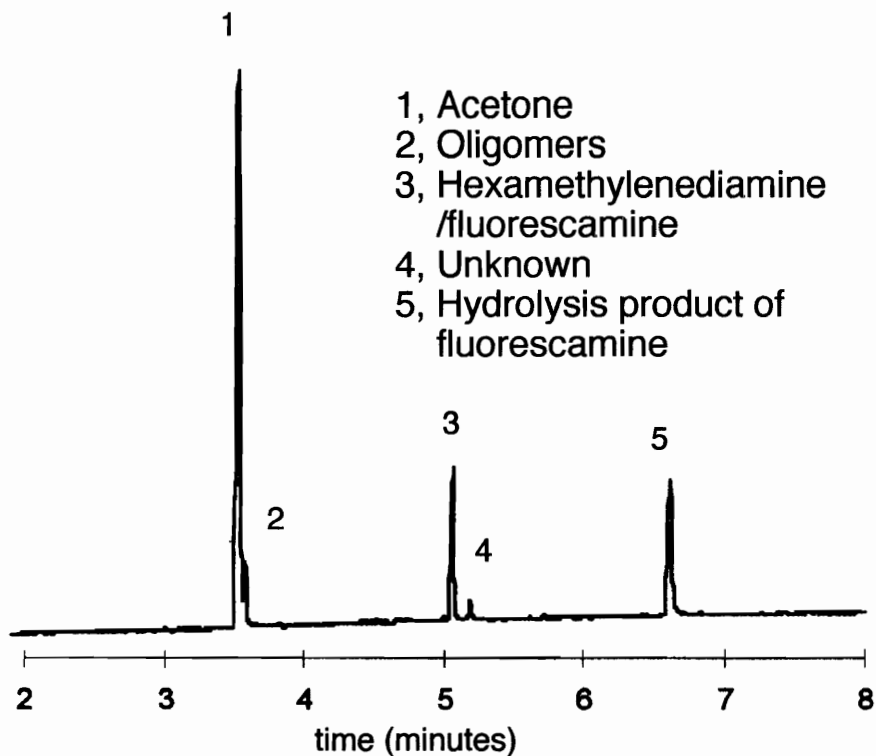


Figure 39. Electropherogram of nylon 6/6 with fluorescamine.

Condition: 75 mm x 57 cm capillary (Ld = 50 cm); +15 kV applied Voltage; 50 mM borate buffer, pH = 9.2; temperature 25 °C; injection: 3 psi for 2 seconds; wavelength = 280 nm. Beckman P/ACE 2100 instrument.

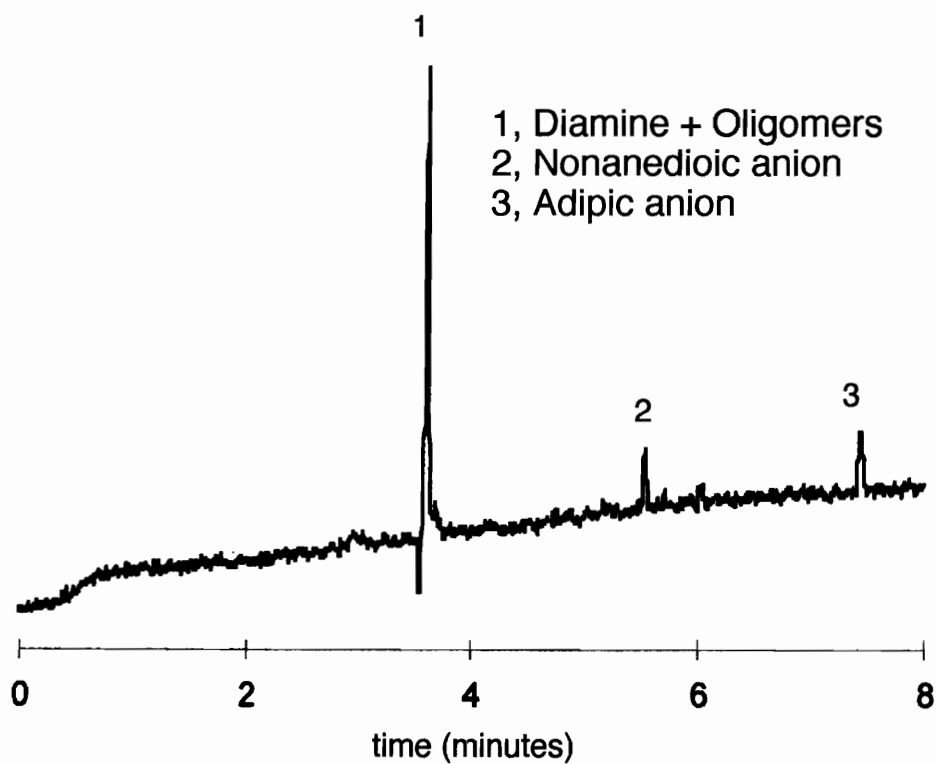


Figure 40. Electropherogram of a mixture of nylon 6/6 and 6/9 without derivatization. Condition: 75 mm x 57 cm capillary (Ld=50 cm); +15 kV applied Voltage; 50 mM borate buffer, pH=9.2; temperature 25 °C; injection: 3 psi for 2 seconds; wavelength=200 nm. Beckman P/ACE 2100 instrument.

3.2.4. The Analysis of Nylon 11 and Nylon 12

The decompositions of nylon 11 and 12 produce only ω -amino-carboxylic acids. In a borate buffer (pH = 9.2), they can be easily separated by CZE because they have same charge but different molecular size. But they are very difficult to detect due to the lack of a UV chromophor. After derivatization with fluorescamine, they can be easily separated and detected by CZE. Figure 41 shows the separation of a mixture of the hydrolysis products of nylon 11 and nylon 12 after derivatization with fluorescamine. Peak 1 is acetone, peak 2 is the derivative of nylon 12 with fluorescamine, and peak 3 is the derivative of nylon 11 with fluorescamine. Peak 4 is from fluorescamine. The derivatized products of nylon 11 and nylon 12 show good separation under these experimental conditions.

Figure 42 shows the separation of the derivatives of a mixture of nylon 66, nylon 11 and nylon 12 with fluorescamine. Peak 1 is acetone and peak 2 is the proposed oligomers, which appear in nylon 66. Peak 3 is the derivative of hexamethylenediamine and peak 4 is an impurity. Peak 5 and 6 are the derivatives of ω -aminododecanoic acid and ω -aminoundecanoic acid from nylon 12 and nylon 11, respectively. Peak 7 is the hydrolysis product of fluorescamine. The most significant thing from this electropherogram is that we can separate different amine monomers by CZE if they co-exist in the product.

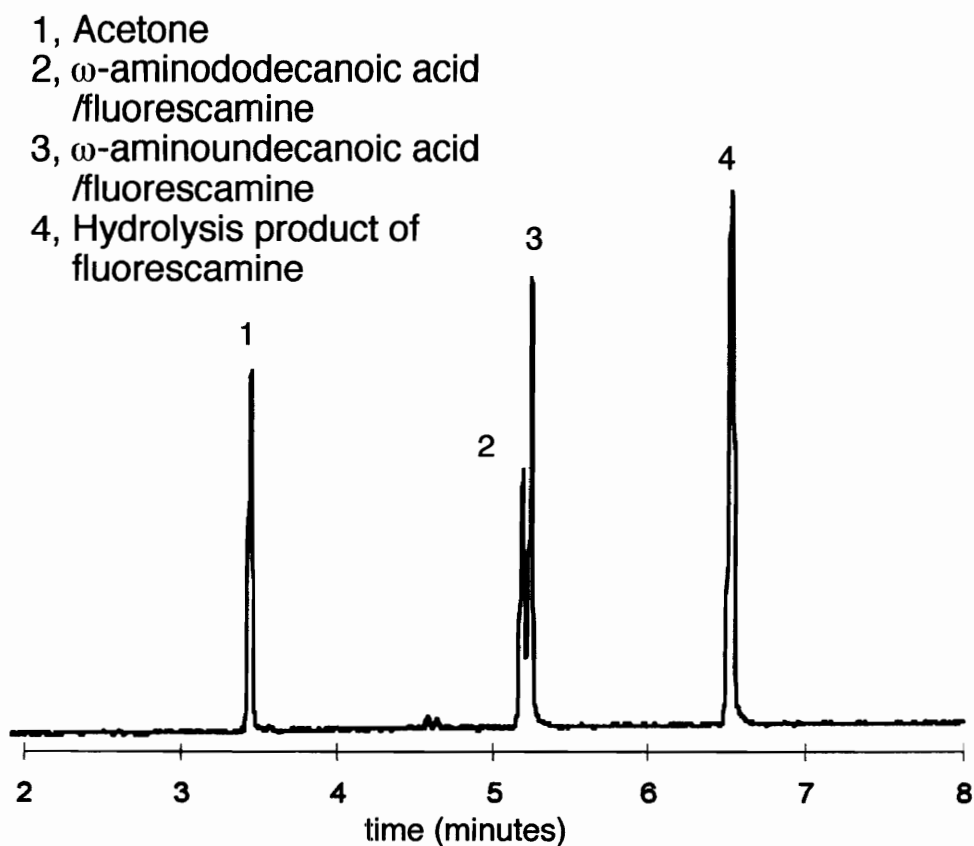


Figure 41. Electropherogram of a mixture of nylon 11 and 12 with fluorescamine. Condition: 75 mm x 57 cm capillary (Ld = 50 cm); +15 kV applied Voltage; 50 mM borate buffer, pH = 9.2; temperature 25 oC; injection: 3 psi for 2 seconds; wavelength = 280 nm. Beckman P/ACE 2100 instrument.

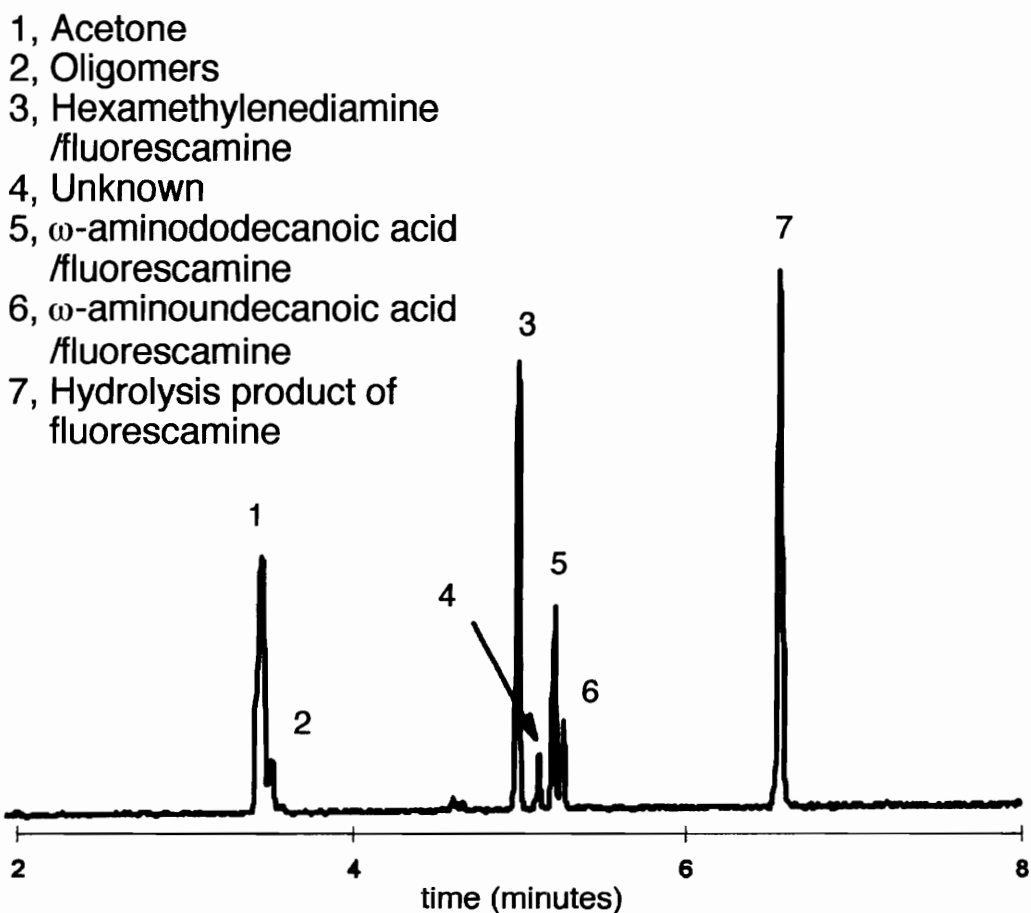


Figure 42. Electropherogram of a mixture of nylon 6/6, 11 and 12 with fluorescamine. Condition: 75 mm x 57 cm capillary (Ld = 50 cm); +15 kV applied Voltage; 50 mM borate buffer, pH = 9.2; temperature 25 oC; injection: 3 psi for 2 seconds; wavelength = 280 nm. Beckman P/ACE 2100 instrument.

3.2.5. The Analysis of an Industrial Nylon

One application of this method was to analyze an industrial nylon sample. The impurity to be analyzed was bis(hexamethylene)triamine (BHMT) and the amount of this impurity was about 0.01 percent. It is a triamine, basic and very polar. It can not be directly analyzed by GC without derivatization. There are 5 active hydrogen atoms in this molecule which need to be derivatized before the analysis. As pointed out earlier, the derivatization of this amine with a silylation reagent will produce several products due to steric hindrance. The ratio of these products is dependent on the reaction time, reaction temperature, and the ratio of the reactants. It is very difficult to obtain an identical ratio of these products run after run. That means it is unreliable to use just one of these products to quantify BHMT in the product.

By using CZE, this problem can be solved with the combination of the simple derivatization of the primary and second amines with fluorescamine and the high resolution power of CZE. Without derivatization, the separation of the decomposition products gives only one peak (Figure 43). From the migration time, we know it is an anion, either a terephthalate or isophthalate anion. There is no peak at t_0 . Thus there is no neutral species. That gives us the information that the product was possibly made from an aliphatic diamine with an aromatic diacid. Figure 44 shows the separation of derivatives of a standard solution, hexamethylenediamine and BHMT, with fluorescamine. The derivatives of these two amines are well separated. The derivative of BHMT eluted later since it has three negative charges while that of hexamethylenediamine has only two negative charges. Figure 45 shows the separation of the derivatives of

hydrolysis products of the industrial nylon. In addition to acetone, fluorescamine and terephthalate peaks, there are three amine peaks, all well separated.

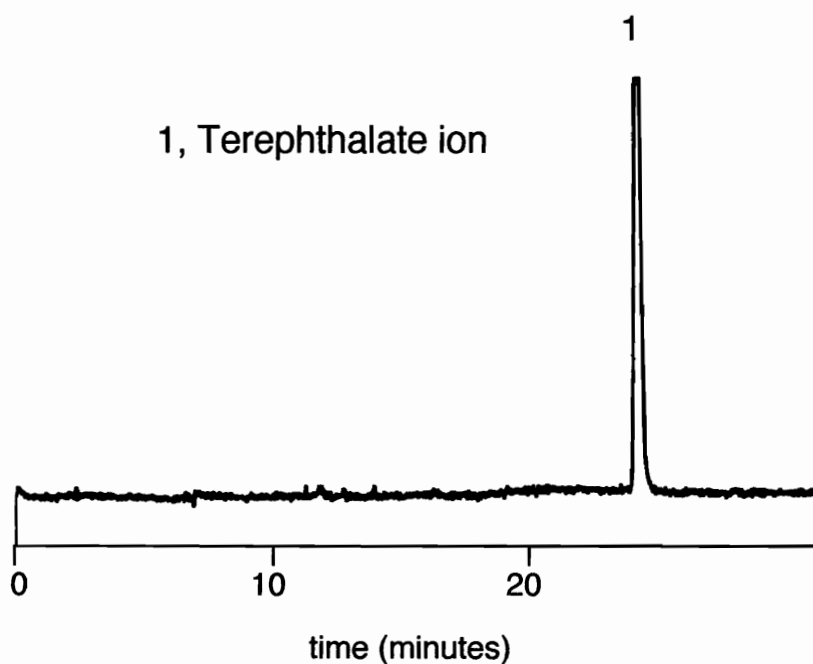


Figure 43. Separation of the industrial nylon without derivatization. Experiment was performed in home made system. Condition: 75 mm x 61 cm capillary ($L_d = 47$ cm); + 10 kV applied voltage; 75 mM borate buffer, pH = 9.2; detection wavelength, 280 nm.

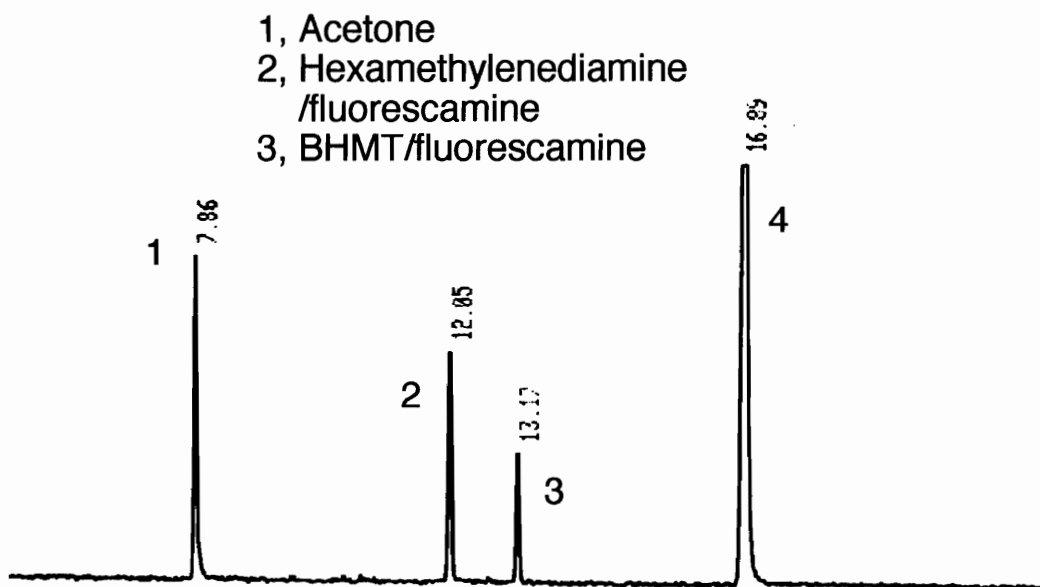


Figure 44. Separation of the derivatives of hexamethylenediamine and BHMT with fluorescamine. Experimental conditions : 75 mm x 61 cm capillary (Ld = 47 cm); + 10 kV applied voltage; 75 mM borate buffer, pH = 9.2; detection wavelength, 280 nm.

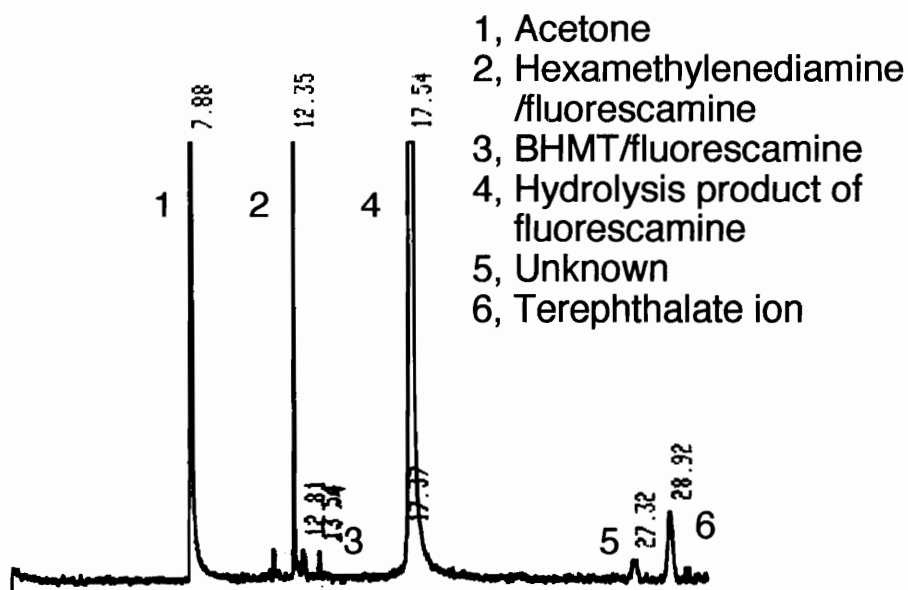


Figure 45. Separation of the derivative of industrial nylon with fluorescamine. Experimental conditions: 75 mm x 61 cm capillary (Ld = 47 cm); + 10 kV applied voltage; 75 mM borate buffer, pH = 9.2; detection wavelength, 280 nm.

3.3. CZE ANALYSIS OF RANITIDINE IN URINE SAMPLE

3.3.1 Conditions for Separation and Detection of Ranitidine by CZE

Ranitidine is a drug used for the treatment of ulcers. It inhibits gastric acid secretions by inhibiting the action of histamine as its receptor. The structure of Ranitidine is shown in Figure 46.

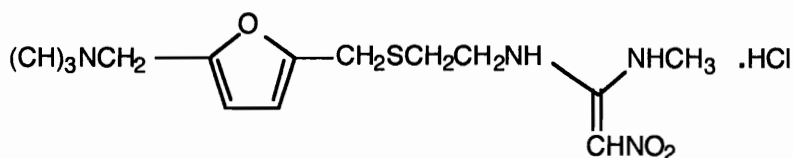


Figure 46. Structure of ranitidine hydrochloride (Zantac®)

It is a basic compound. The analysis of basic drugs can present difficulties in HPLC (124) due to the peak tailing caused by adsorption on the acidic silica surface.. Capillary Electrophoresis is a relatively new analytical technique which is finding increased application within the pharmaceutical industry. The application areas include enantiomer separations, trace analyses(125), drugs in urine (126) and determination of drug purity (127). Chee and Wan (128) separated 17 basic drugs in less than 11 minutes using CZE in a phosphate buffer (pH=2.4). Altria (129) also demonstrated the separation of 11 basic drugs by CE using similar experimental conditions, a phosphate buffer

(pH=3.00) was used. At this pH, the electroosmotic flow is very small. The migration of analytes in the column is dominated by electrophoretic mobilities.

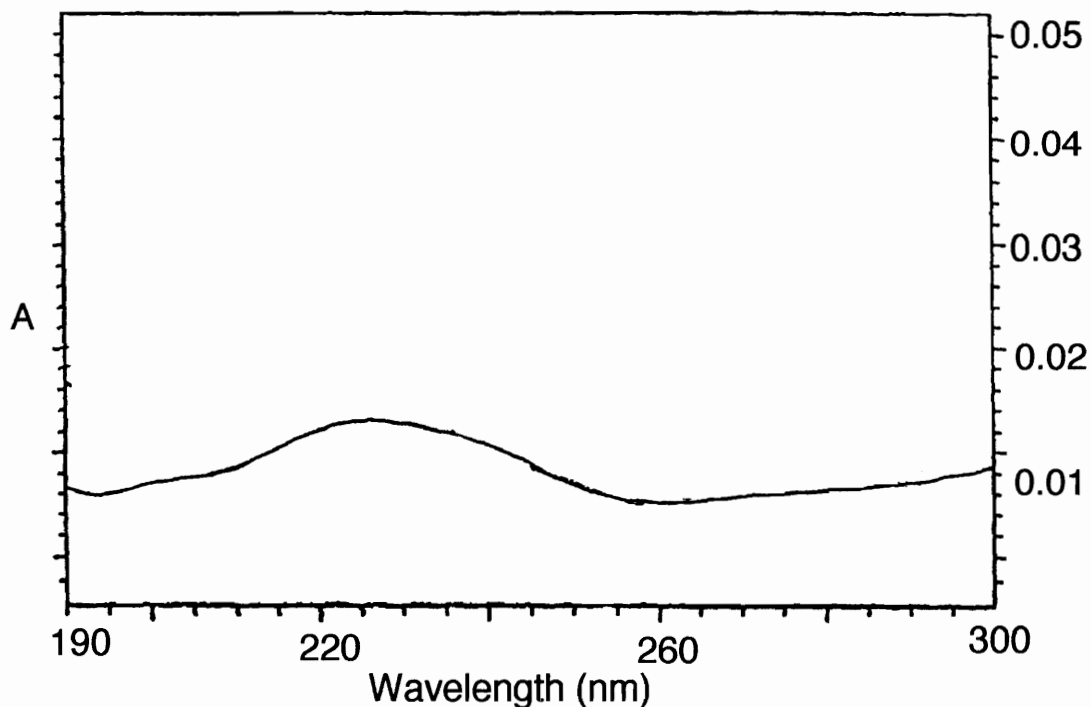


Figure 47. UV spectrum of Ranitidine

From the UV spectrum, we can see that the ranitidine does not show strong UV absorption (Figure 47). The absorption maximum occurs at around 225 nm. The Beckman CE instrument only provides 4 wavelengths, 200, 214, 254 and 280 nm. So 214 nm was chosen for this work. Figure 48 shows the electropherogram of 100 ppm ranitidine in a phosphate buffer solution (pH=3).

A calibration curve made using 20, 40, 60, 80 and 100 ppm of ranitidine hydrochloride in deionized, double distilled water, is shown in Figure 49. The peak height was used . The linearity of this plot is 0.999.

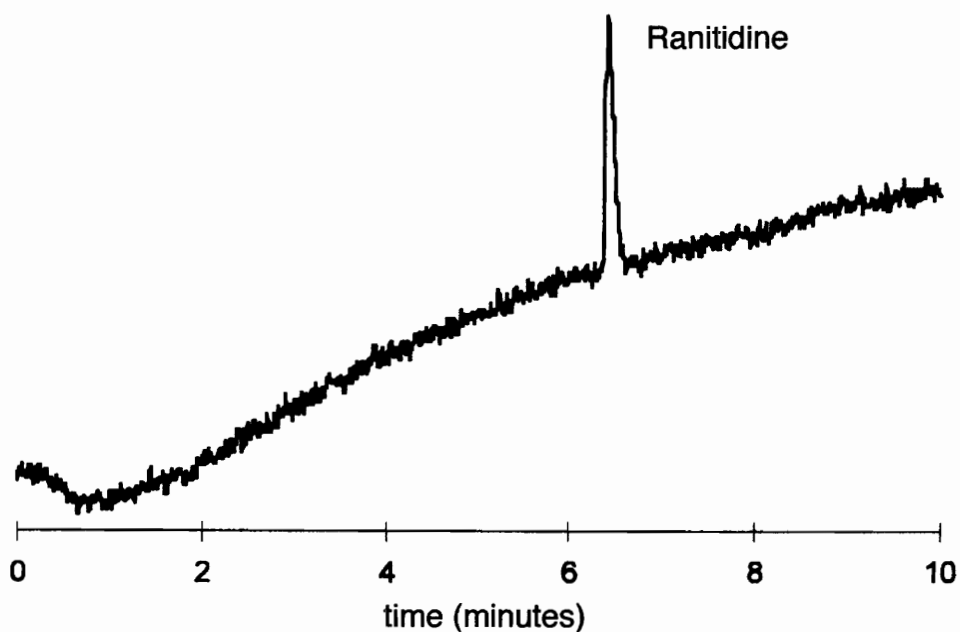


Figure 48. Electropherogram of 100 ppm ranitidine in phosphate buffer solution. Conditions: Beckman P/ACE 2100 instrument; Column: 57 cm x 75 μ m (Ld = 50 cm); Buffer: 25 mM phosphate, pH = 3.0; Wavelength = 214 nm; 25 $^{\circ}$ C; Injection: 3 psi for 2 sec.

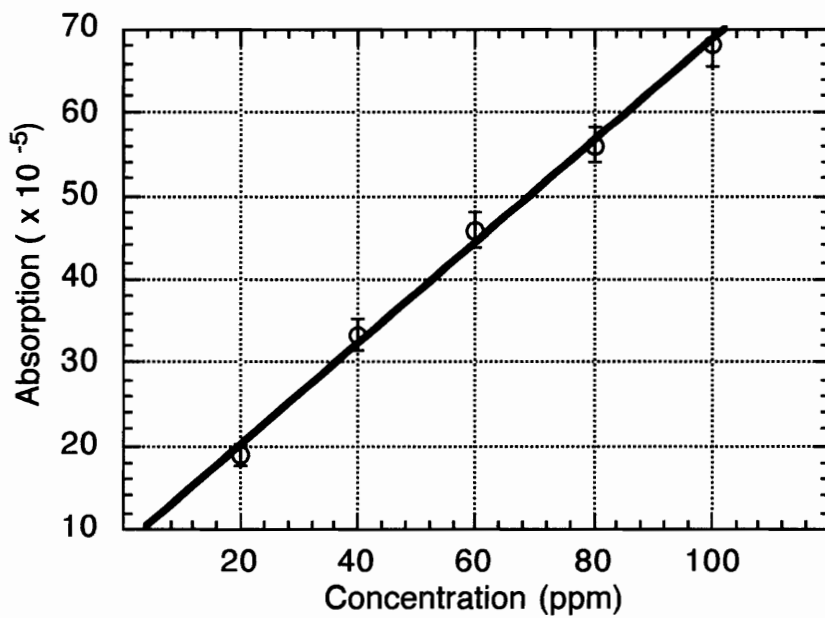


Figure 49. A calibration curve of ranitidine. Eight measurements were performed for each point. Measurement errors (standard derivation) are shown in the Figure.

MDQ (minimum detectable quantity) in CE depends on the internal diameter of the column, the sample volume injected and the detection signal. Under the experimental conditions in this work, MDQ was determined by the injection of 5 ppm ranitidine (3 psi for 2 seconds). The electropherogram is shown Figure 50. The signal of 5 ppm ranitidine is four times the noise level. So the MDQ should be about 3 ppm (two times the noise level).

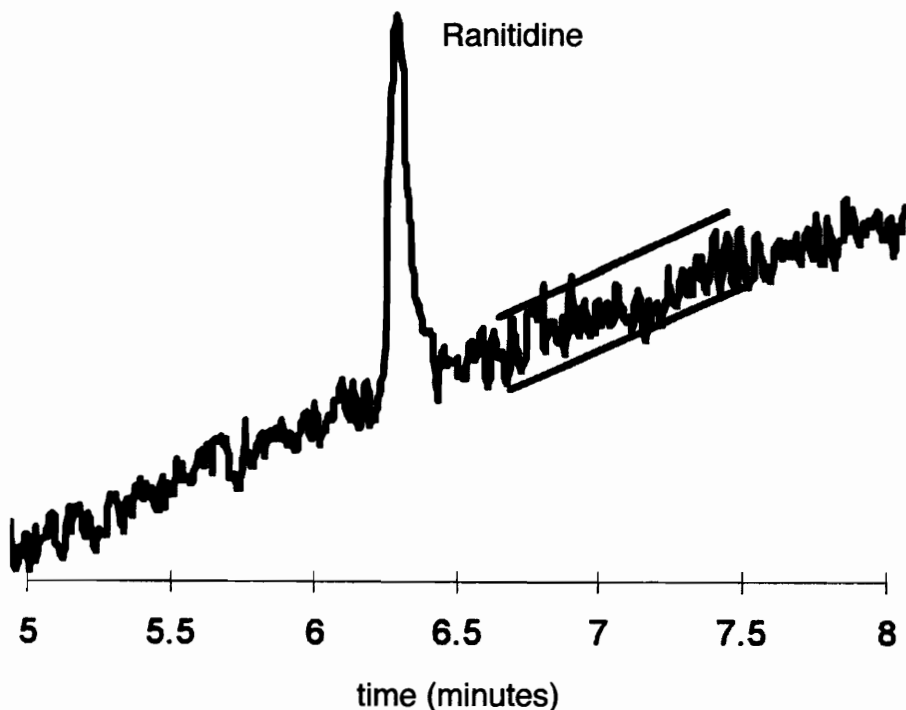


Figure 50. Signal to noise ratio (5 ppm ranitidine).

Conditions: Beckman P/ACE 2100 instrument; Column: 57 cm x 75 μm (Ld = 50 cm); Buffer: 25 mM phosphate, pH = 3.0; Wavelength = 214 nm; 25 $^{\circ}\text{C}$; Injection: 3 psi for 2 sec.

3.3.2 Conditions for Solid Phase Extraction

Solid phase extraction (SPE) was introduced in the 1970s for sample preparation ⁽¹³⁰⁾. Compared to liquid-liquid extraction, it reduces the time required, especially when automated methods are used; it also reduces the solvent consumption and it can be used for very small amounts of sample.

The principle of SPE is the partitioning of sample between two phases, one solid and the other liquid. There are two steps to SPE. The first is the retention (adsorption) step, in which analytes in solution are adsorbed onto the solid phase. The second is the desorption step, in which analytes are desorbed by a strong solvent which has greater affinity for the solid phase than the analytes.

The SPE column used in this work is SPEC® C18AR (Ansys. Inc, Irvine, CA) microcolumn, which is a silica gel bonded with octadecylsiloxane (C18). The retention of analytes to this microcolumn is dominated by dispersion forces (hydrophobic interaction). To ensure that analytes will be retained by the solid phase, the interaction between the analyte and the liquid phase must be minimized. This sometimes can be achieved by adjusting the pH and/or ionic strength of the solution.

One important parameter for SPE columns is the breakthrough volume. This is the sample volume where the analyte starts to elute from the column. This parameter limits the sample volume that can be used in SPE. It is determined by the column capacity for that analyte, and this capacity is influenced by pH, ionic strength, and type of analyte and liquid phase.

As pointed out previously, ranitidine is a basic compound. It exists in a protonated form at relatively low pH. The interaction forces between ranitidine and the liquid phase will be affected by pH. The stronger the interaction between ranitidine and the liquid phase, the less ranitidine will be adsorbed by the solid phase. To investigate the influence of pH on the retention of ranitidine, four solutions with 100 ppm ranitidine at different pH value were prepared. These were phosphate buffers of pH 3, 5.8, and 7.5 and a borate buffer of pH 8.7. Three mL (0.3 mg ranitidine) of each solution was passed through the SPE cartridge; the eluate was collected and analyzed by CE. The percent of ranitidine retained then was calculated. The results are as predicted. At pH 3, only 18% of ranitidine was retained by the SPE cartridge. As the pH increased, the percentage of ranitidine retained increased. When a pH 8.6 borate buffer was used, all the ranitidine (0.3 mg) was retained. Figure 51 shows this relationship.

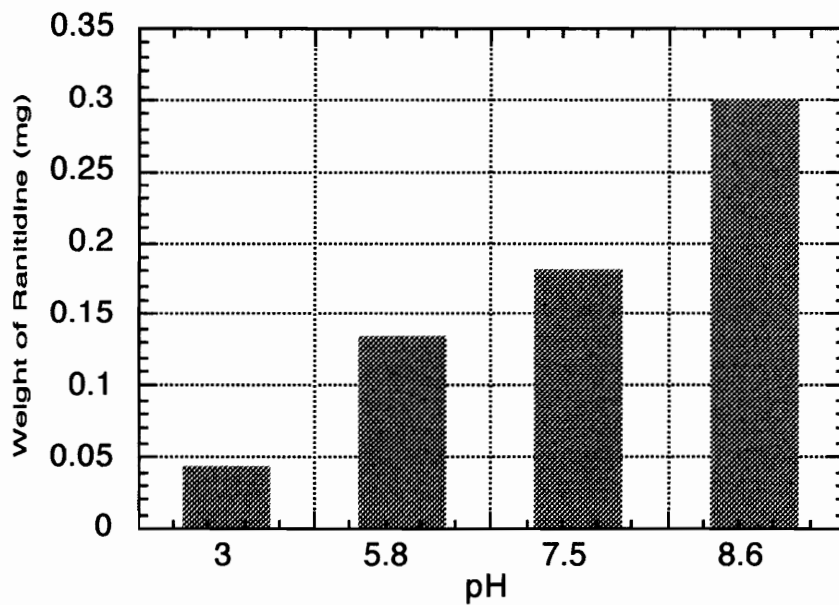


Figure 51 The influence of pH on the retention of ranitidine by SPE.

When 0.3 mg of ranitidine solution (3.0 mL, 100 ppm) was passed through the cartridge. Notice that at pH = 8.6, all ranitidine added were retained by the cartridge.

The desorption of ranitidine from the SPE cartridge was carried out by adding 2 times 0.5 mL methanol to the column. To investigate the recovery of ranitidine by SPE extraction, three mL of 100 ppm ranitidine in a borate buffer (pH=8.7) were added to the SPE cartridge. Then two mL of methanol were added to the column to desorb the ranitidine; the eluate was collected in a clean test tube. After removing the methanol, four mL of phosphate buffer (pH=3.0) were added. The solution was analyzed by CZE to determine the amount of ranitidine recovered. Five experiments were carried out and the results are shown in the Table 2. The experimental results shows that good recovery was found under these experimental conditions.

Table 2. Recovery of Ranitidine from Water (n = 6).

	Trial 1	Trial 2	Trial 3	Trial 4	Trial 5
Added (mg)	0.30	0.30	0.30	0.30	0.30
Found (mg)	0.28	0.29	0.32	0.27	0.31
% Recovery	93%	97%	107%	90%	103%
% RSD	8.5%	9.6%	6.5%	10 %	12 %

3.3.3 Extraction of Ranitidine from Spiked Urine Sample

It has been reported that about 30% of the dosage (300 mg per day) of ranitidine is discharged without being metabolized ⁽¹³¹⁾. Assuming that an average person excretes 4 liters of urine a day, the concentration of ranitidine would be 22.5 ppm from a 300 mg dosage. It is calculated that about 0.06 mg of ranitidine could be expected in a 3 ml urine sample. The capacity of this SPE cartridge is sufficient to quantitatively extract ranitidine from the urine sample if the basic conditions are used.

An electropherogram of a urine sample spiked with 50 ppm ranitidine before extraction is shown in Figure 52. There is interference of the ranitidine peak from other compounds. The pH of the sample was adjusted to 8.5 by adding 1 M NaOH before loading the sample to the SPE cartridge. After passing 3 mL of urine sample through the SPE cartridge, the cartridge was washed with 2 mL of deionized water. After desorption with 2 mL of methanol, the eluate was analyzed by CE. The electropherogram (Figure 53) shows that no interference with the ranitidine peak. From these two electropherograms, it can be seen that SPE is a good method to extract ranitidine from the urine.

The quantitation results were performed by examining 5 urine samples spiked with 50 ppm ranitidine. The results are summarized in Table 3. The recovery of ranitidine from urine sample was from 80% -113%, and %RSD ranged from 8.7% to 15% based on 6 analyses.

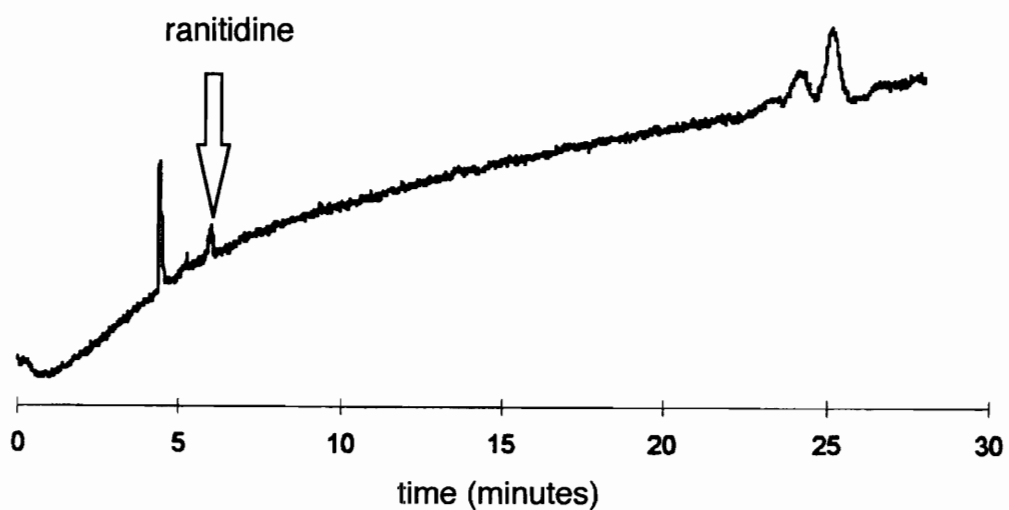


Figure 52. Electropherogram of a urine sample spiked with ranitidine before extraction. Conditions: Beckman P/ACE 2100 instrument; Column: 57 cm x 75 μ m (Ld = 50 cm); Buffer: 25 mM phosphate, pH = 3.0; Wavelength = 214 nm; 25 °C; Injection: 3 psi for 2 sec.

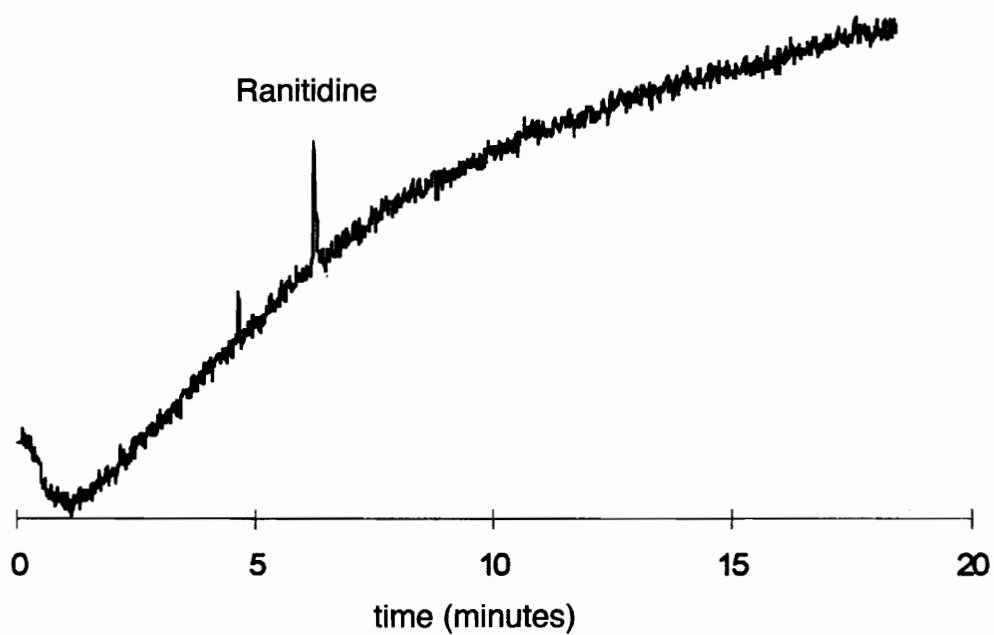


Figure 53. Electropherogram of ranitidine desorption from SPE cartridge.
Conditions: Beckman P/ACE 2100 instrument; Column: 57 cm x 75 μ m (Ld = 50 cm); Buffer: 25 mM phosphate, pH = 3.0; Wavelength = 214 nm; 25 $^{\circ}$ C; Injection: 3 psi for 2 sec.

Table 3. Recovery of Ranitidine from Spiked Urine Sample.

SAMPLE	1	2	3	4	5
Added (mg)	0.15	0.15	0.15	0.15	0.15
Found (mg)	0.15	0.14	0.17	0.12	0.16
Recovery (%)	100 %	93 %	113 %	80 %	107 %
% RSD	12 %	8.7 %	11 %	15 %	9.2%

3.4. NON AQUEOUS CE

The performance of classic electrophoresis in non-aqueous solvents has been known for long time ⁽¹³²⁾. Non-aqueous solvents showed advantages in some specific applications, especially for the separations of compounds that are not soluble in water and that have a similar mobility in aqueous solution.

In CE analysis, organic solvents are often added to the buffer solution to increase the solubility of organic compounds. It has also been demonstrated⁽¹³³⁾ that adding organic modifiers to the CZE buffer may improve the resolution. This enhancement in performance is explained by the fact that organic solvents change viscosity and dielectric constant of the solution buffer, as well as the zeta potential of the capillary wall ⁽¹³⁴⁾. Typically, organic modifiers are less than 30% (volume) of the separation buffer. MECC is also widely used for hydrophobic compounds analyses.

Non-aqueous CE is another alternative for the analysis of hydrophobic compounds, especially, when on-line CE-MS is performed. MS systems are usually not compatible with non-volatile buffers or surfactants. Though Jorgenson et al. ⁽¹³⁵⁾ reported a separation of quinolines in 100% acetonitrile as early as in 1984, this area has been ignored by most CE workers. Recently, there have been several papers about non aqueous CE separations. Khaledi et al. ⁽¹³⁶⁾ reported separation of six peptides in formamide solvent. Naylor et al. ⁽¹³⁷⁾ reported the analysis of drug metabolites using on-line CE-MS in a mixture of ammonium acetate , methanol, and acetic acid. Cassidy et al. ⁽¹³⁸⁾ reported the analysis of inorganic anions in a mixture of dimethylformamide

and triethyleamine. There are other reports ^(139, 140) using organic solvents in CE separation.

As previously discussed, the electroosmotic mobility (μ_{e0}) is expressed as:

$$\mu_{e0} = \varepsilon\zeta/\eta \quad (15)$$

where μ_{e0} is electroosmotic mobility, ζ is the zeta potential of the capillary wall and ε , and η are the dielectric constant and viscosity of the solution. Electroosmotic mobility is proportional to the ratio of ε/η .

Table 4 shows some physical properties ⁽¹⁴¹⁾ of some candidate organic solvents for CE. Comparing the ratio of ε/η of these solvents with water, it can be seen that N-methylformamide (NMF) is a good candidate. It has a high boiling point (182°C); this minimizes the evaporation of solvent at room temperature. Also, it possesses a high dielectric constant and low viscosity. Chemically, it is a basic compound, so the ionization of silanol groups of the capillary wall in this solvent is possible. Considering all these factors, it is a good solvent for electroosmotic flow.

Table 4. Physical Properties of Some Organic Solvents for CE

Solvent	bp (°C)	Viscosity (cP, 25 °C)	Dielectric constant
Water	100	0.89	80
Formamide	210	3.3	111
N-methyl formamide	153	0.80	182
Dimethyl sulfoxide	189	1.1	45

3.4.1 N-Methylformamide as an Non-Aqueous Solvent for CE separation

In pure NMF (used as purchased) solvent, the electroosmotic mobility is measured by using toluene as an indicator (Figure 54). At an applied electric field of 350 V/cm, the electroosmotic mobility is $6.2 \times 10^{-4} \text{ cm}^2 \text{ V}^{-1} \text{ sec}^{-1}$, which is close to that in a basic aqueous buffer. This implies that there is a significant zeta potential on the capillary wall. This phenomenon can be explained by the ionization of the silanol groups in basic NMF solvent. The pKa of silanol groups of the capillary wall range from 2 to 5 depending on their existing form. The high dielectric constant of NMF also favors high electroosmotic flow. The current under experimental conditions in NMF solvent is only 7.6 μA , which is well below that of a 50 mM borate buffer under the same experimental condition (which is 30 μA in this instrument). This implies that high voltage is possible for NMF media to achieve fast separation without Joule heating problem.

A mixture of carboxylic acids was used to evaluate this non-aqueous solvent. Figure 55 shows the structures of these compounds. Toluene was used for the indication of EOF. Figure 56 shows the separation of a mixture of 5 compounds in pure NMF solvent. These compounds are well separated. The last peak, trimellitic acid, elutes in 6 minutes. It takes about 17 minutes for trimellitic acid to elute if the separation is performed in 50 mM borate buffer solution (pH=10) with the same voltage ⁽¹⁴²⁾. The efficiency, reproducibility of both migration time and peak area of these compounds are summarized in Table 5. Reproducibility of migration time is good, but peak areas are poor. A relatively high efficiency is obtained for these analyses (n=6).

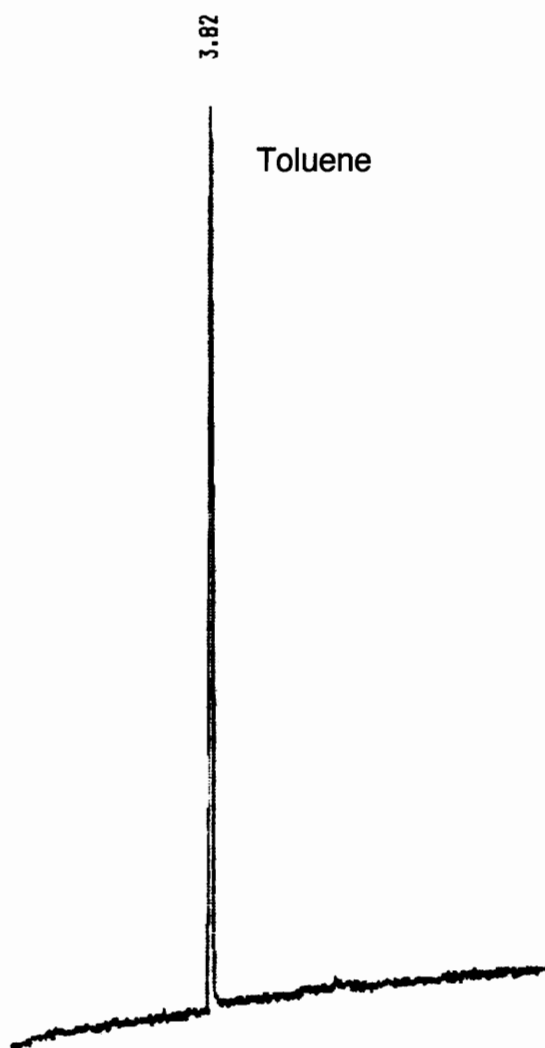
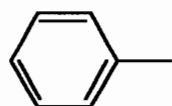
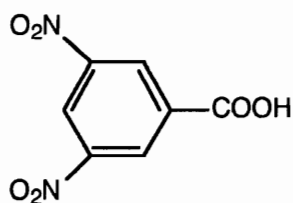


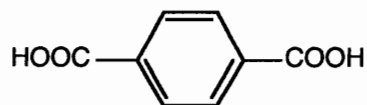
Figure 54. Measurement of electroosmotic flow in pure NMF media.
Experimental conditions: Column: 57 cm x 75 μm ($L_d = 50$ cm);
Wavelength = 280 nm; Analyte: toluene; Injection: 2 sec 3 psi;
Instrument: Beckman P/ACE 2100. Voltage: 20 kV; Current: 7.6 μA .



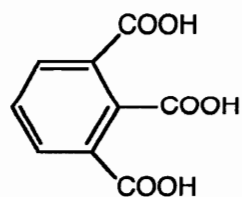
Toluene



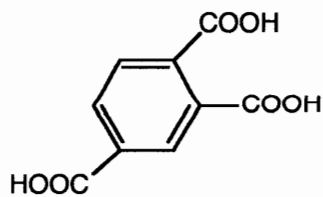
Dinitrobenzoic acid



Terephthalic acid



Hemimellitic acid



Trimellitic acid

Figure 55. Structures of compounds used for NMF evaluation.

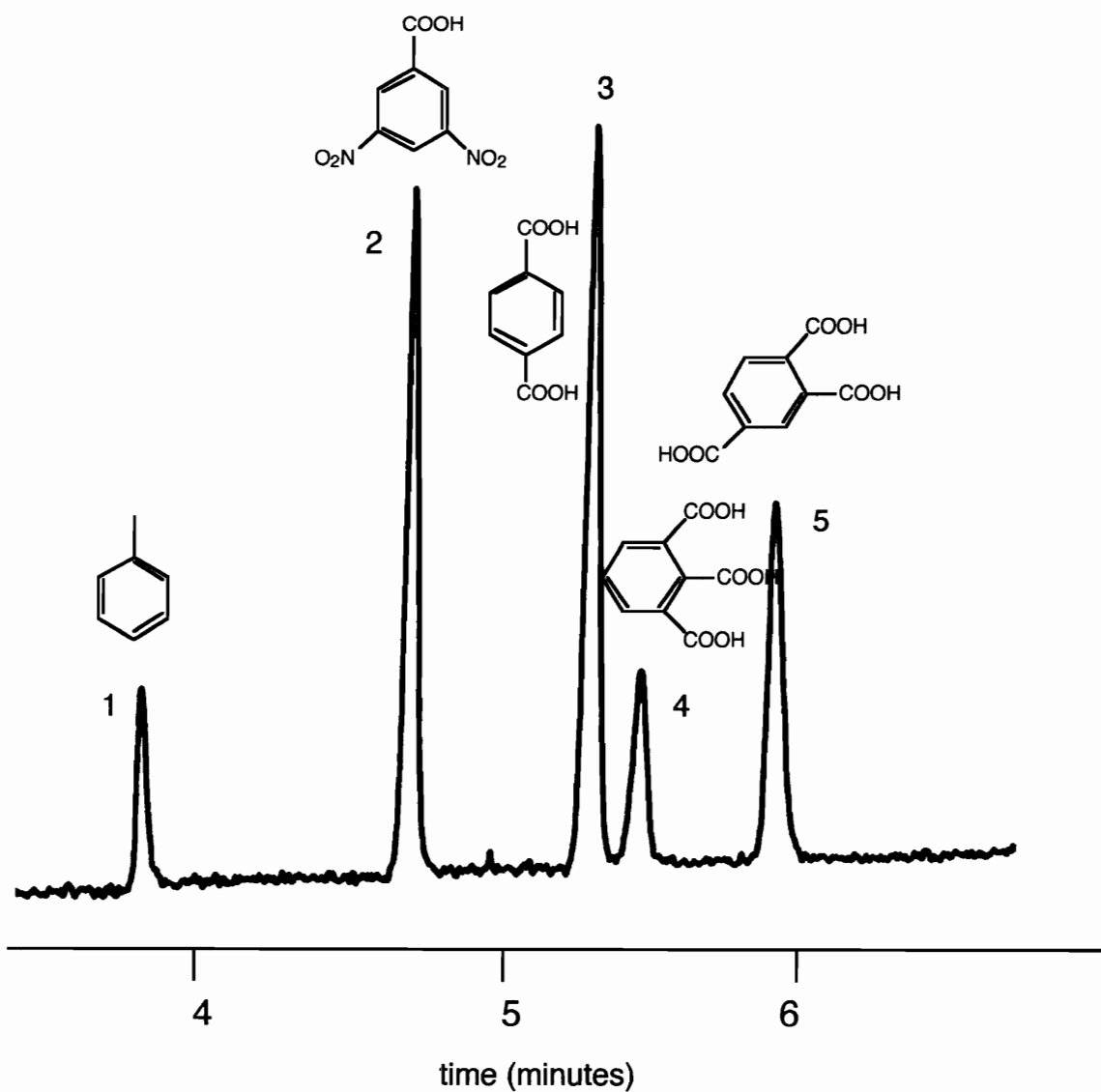


Figure 56. Typical electropherogram of 5 compounds in pure NMF solvent. Experimental conditions: Column: 57 cm x 75 μ m (Ld = 50 cm); Wavelength = 280 nm; Injection: 2 sec 3 psi; Instrument: Beckman P/ACE 2100. Voltage: 20 kV.

Table 5. The Efficiency and Reproducibility of Migration Times and Peak Areas of Analytes in NMF solvent. Experimental conditions are the same as in Figure 56. %RSDs are calculated from 6 runs.

Compounds	% RSD (tm) (n = 6)	%RSD (Area) (n = 6)	Efficiency (N) (x 10 ³)
Toluene	0.8 %	12%	17
Dinitro benzoic acid	1.0%	8.5%	16
Terephthalic acid	1.2%	10%	15
Hemimellitic acid	0.9%	14%	15
Trimellitic acid	0.7%	9.2%	14

3.4.2 The Influence of the percentage of DMSO on separation

DMSO is a good organic solvent, in which most of organic compounds are soluble. But DMSO has a low dielectric constant and high viscosity. So it is interesting to see the behavior of a mixture of NMF and DMSO as an organic medium for CE analysis. The influence of %DMSO (v/v) on the electrophoretic mobilities of these compounds is shown in Table 6. The electrophoretic mobility of toluene indicates the electroosmotic flow in these solvents. The electroosmotic mobility decreases with increasing DMSO percentage. However the electroosmotic mobility is large enough ($4.0 \times 10^{-4} \text{ (cm}^2 \text{ s}^{-1} \text{V}^{-1})$) for the separation even 40% DMSO (v/v) was added. The electric current in 40% DMSO (v/v) solvent is small ($4.5 \mu\text{A}$) and stable. By contrast, in aqueous solution in 40% of organic modifier produces an unstable current (138). The electrophoretic mobilities of other acids did change as DMSO was added. However, there were no significant differences in the electrophoretic mobilities up to 20% DMSO (v/v).

NMF is a toxic compound. Caution should be taken while handling this compound. NMF is a basic compound; only acidic compounds can be separated in this solvent. The UV cutoff wavelength of NMF is 250 nm. This limits NMF for some analyses using a UV detector. However, if an on-line MS detector is used, NMF will be a good solvent to do acidic compounds analyses.

Table 6. The Influence of %DMSO (v/v) on the Electrophoretic Mobilities of Analytes. (Unit: $\text{cm}^2 \text{s}^{-1} \text{V}^{-1}$)

Compounds	Pure NMF	10%DMSO in NMF (v/v)	20%DMSO in NMF (v/v)	40%DMSO in NMF (v/v)
Toluene	6.2	5.6	5.0	4.0
Dinitro benzoic acid	1.52	1.51	1.53	1.60
Terephthalic acid	2.05	2.09	2.01	2.14
Hemimellitic acid	2.23	2.29	2.27	2.22
Trimellitic acid	2.31	2.38	2.35	2.41

CHAPTER IV. CONCLUSIONS

The focus of this research was exploration of new applications of CZE. Four different methods have been studied in this work.

A method was developed for polyimide composition analysis. The polyimide was decomposed to its corresponding monomers by sodium hydroxide at high temperature inside a sealed glass tube. The decomposition products were analyzed by CZE. Since there are no derivatization and separation steps needed, it is much simpler than the existing fusion reaction chromatography method. The decomposition of some monomers was also observed. Though it is impossible to identify all peaks in the electropherogram, it is still possible to use the electropherogram to elucidate the composition of the polyimide. Different polyimides give different electropherograms and the same monomer in different polyimides gives the same pattern in electropherograms under the same reaction conditions. A pattern of an electropherogram can be viewed as a "finger print" of a polyimide, or more precisely, the pattern (in part) of an electropherogram is a "finger print" of a monomer. Through identifying these "finger prints" in an electropherogram, it is possible to learn the composition of the polyimide.

For nylon composition analysis, the developed method is simple and easy to use. Nylon was hydrolyzed by hydrobromic acid at 150 °C. The amines were analyzed after derivatization with fluorescamine. The acids were analyzed directly and detected by a UV detector at a wavelength 200 nm. There is no separation step necessary. The hydrolysis conditions are much milder than that used in pyrolysis GC. There are no decomposition reactions of

monomers observed. This method is ideal for complete compositional analysis of nylon. It has also been demonstrated that the analysis of trace amounts of amine impurities is possible. Such analysis is very difficult by other methods.

The method developed should be suitable for other kinds of condensation polymer analysis, especially for crystalline and semicrystalline polymer (polyester) compositional analysis. These polymers are made from aromatic acids and phenols. The decomposition products from these polymers are ideal for analysis by CE without any derivatizations or pre-separations.

Drug analysis is another rapidly expanding area of CE applications. In this work, a method was developed to extract and analyze ranitidine, Zantac[®], in urine samples. The conditions for the solid phase extraction of ranitidine from water and urine samples were optimized. A high pH was found good for the extraction. The CZE analysis of ranitidine is simple and fast. Good recovery and a reasonable reproducibility were obtained in this work.

NMF and a mixture of NMF and DMSO as a non-aqueous solvent for CE analysis were tested in this work. The electroosmotic flow in these solutions is large and the electric current is low. This makes it possible to use a high voltage for a fast analysis. In addition, the low volatility of NMF and the low current also make it possible to connect CE to an on-line ion spray mass spectrometry (ISP-MS) detector. The separation of a mixture of aromatic acids in these solvents were studied. The analysis time is much shorter than that in a borate buffer solution. The high UV cutoff wavelength of NMF limits its application when a UV detector is used. However, this solvent should be good for acidic and hydrophobic compounds analyses if an on-line MS detector is used.

REFERENCES

1. H. McNair, X Sun, *JHRC*, **18**, 115, 1995.
2. X. Sun, H. McNair, The Pittsburgh Conference, New Orleans, March 6-10, 1995
3. H. McNair, X. Sun, *Electrophoresis*, Accepted, .
4. X. Sun, D. Blackman, H. McNair, 17th International symposium on Capillary Chromatography and Electrophoresis, Wintergreen VA, May 7-11, 1995.
5. H. McNair, X. Sun, 17th International symposium on Capillary Chromatography and Electrophoresis, Wintergreen VA, May 7-11, 1995
6. P. H. O'Farell, *J. Biol. Chem.*, **250**, 4007, 1975.
7. R. Virtanen, *Acta Polytech. Scand. Appl. Phys. Ser. (Helsinki)*, **123**, 1974.
8. F. E. P. Mikkers, F.M. Everaerts, and T.P.E. Verheggen, *J. Chromatogr.*, **169**, 11, 1979.
9. J. Jorgenson, K. D. Lukacs, *Anal. Chem.*, **53**, 1298, 1981.
10. J. Jorgenson, K.D. Lukacs, *Science*, **222**, 226, 1983.
11. Y. Wahlbroehl, J. Jorgeson, *J. Chromatogr.*, **315**, 135, 1984.
12. E. Moring, T.T. Reel, and R.E.J. Van Soest, *Anal. Chem.*, **65**, 3454, 1993.
13. W. Beck, R. Van Hoek, and H. Engelhardt, *Electrophoresis*, **14**, 540, 1993.
14. X.C. Huang, M.A. Quesada, and R.A. Mathies, *Anal. Chem.*, **64**, 967, 1992.
15. J. Liu, O. Shirote, and M. Novotny, *Anal. Chem.*, **63**, 413, 1991.
16. W.G. Kuhr, E.S. Yeung, *Anal. Chem.*, **60**, 1832, 1988.
17. J. S. Green, J. Jorgeson, *J. Chromatogr.*, **352**, 337, 1986.
18. R. A. Wallingford, A. G. Ewing, *Anal. Chem.*, **61**, 1642, 1989.
19. N. Avdalovic, C. A. Pohl, R.D. Rocklin, and J.R. Stillian, *Anal. Chem.*, **65**, 1470, 1993.
20. C. Chan, M. D. Morris, *J. Chromatogr.*, **540**, 355, 1990.
21. J. S. L. Pentony, R. Zare, and J. Quint, *Anal. Chem.*, **62**, 900, 1990
22. J. Cai, J. Henion, *J. Chromatogr.*, **703**, 657, 1995
23. R. D. Smith, J. H. Wahl, D. R. Godlett, and S.A. Hofstadler, *Anal. Chem.*, **65**, 574A, 1993.
24. J. B. Feen, M. Mann, C. K. Meng, S.F. Wong, and C.M. Whitehouse, *Science*, **246**, 64, 1989.
25. R. D. Smith, C. J. Barinaga, and H. R. Uolseth, *Anal. Chem.*, **60**, 1948, 1988.
26. J. Varghese, R. B. Cohe, *J. Chromatogr.*, **652**, 369, 1993.
27. G. J. M. Bruin, A. C. Van Asten, X. Xu, and H. Poppe, *J. Chromatogr.*, **608**, 97, 1992
28. Y. Ma, R. Zhang, *J. Chromatogr.*, **635**, 341, 1992.
29. C.T. Wang, R. A. Hartwick, *J. Chromatogr.*, **589**, 307, 1992.
30. J. P. Romano, J. Krol, *J. Chromatogr.*, **640**, 403, 1993.
31. R. A. Carpro, R. Mariscal, and J. Welch, *Anal. Chem.*, **64**, 2123, 1992.

- 32 K. Salmon, D. S. Burg, and J. C. Helmer, *J. Chromatogr.*, **549**, 375, 1991..
- 33 J. Snopek, H. Soini, M. Novotny, K.E. Smolknova, and I. Jelinek, *J. Chromatogr.*, **559**, 215, 1991.
- 34 W.C. Brumley, *J. Chromatogr.*, **603**, 267, 1992.
- 35 E. Gassman, J. E.Kuo, and R.N. Zare, *Science*, **230**, 813,1985.
- 36 L. Cellai, C. Desiderio, R. Filippetti, and S. Fanali, *Electrophoresis*, **14**, 823, 1993
- 37 P. D. Grossman, K. J. Wilson, G. Petrie, and H.H. Lauer, *Anal. Biochem.*, **173**, 265, 1988.
- 38 P. D. Grossman, J. C. Colburn, and H.H. Lauer, *Anal. Biochem.*, **179**, 28, 1989.
- 39 A. K. Cobb, M. V. Novotny, *Anal. Chem.*, **64**, 879, 1992.
40. M. J. Gordon, K. J. Lee, A. A. Arias, and R. N. Zare, *Anal. Chem.*, **63**, 69, 1991.
- 41 M. Zhu, T. Wehr, V. Levi, R. Rodriguez, K. Schiffer, and Z.A. Cao, *J. Chromatogr.*, **652**, 119, 1993.
- 42 G. Mandrup, *J. Chromatogr.*, **604**, 267, 1992.
- 43 R. Vincentelli, N. Bihoreau, *J. Chromatogr.*, **641**, 383, 1993.
- 44 G.H. Bolt. *J. Phys. Chem.*, **61**, 1166, 1957.
- 45 R. D. Smith, J. A. Olivers, N.T. Nguyen, and H. R. Uolseth, *Anal. Chem.*, **60**, 436, 1988.
- 46 K.A. Cobb, V. Dolmk, M. Novotny, *Anal. Chem*, **62**, 2478, 1990.
- 47 D. Schmalzing, C.A. Piggee, F. Forest, E. Carrilho, and B.L. Karger, *J. Chromatogr.*, **652**, 149, 1993.
- 48 S. Hjerten, K. Kubo, *Electrophoresis*, **14**, 396, 1993.
49. S. Hjerten, *Chromatogr. Rev.*, **9** , 122, 1967
50. J.H. Knox, *Chromatographia*, **26**, 329 ,1988.
51. S. Hjerten, *Electrophoresis*, **11**, 665 (1990))
51. Y. Kurosu, K. Hibi, T. Sasaki, and Mi. Saito, *HRCC&CC*, **14**, 200, 1991.
52. R.J. Nelson, A. Paulus, A.S. Cohen, A. Guttman, and B.L.Karger, *J. Chromatogr.*, **480**. 111. 1989.
- 53 S. Terabe, K. Otsuka, K. Ichikawa, A. Tsuchiya, and T. Audo, *Anal. Chem.*, **56**,111,1984
- 54 W.L. Hinze, D.W. Armstrong, Eds., American Chemical Society, Washington. D.C. 1987.
- 55 S. Yang, M.G.Khaledi, Pittsburgh Conference, New Orleans, LA. March 6-10, 1995
- 56 E.W. Tsai, M.M. Sigh, H. H. Lu, D. P. Ip, and M. A. Brooks, *J. Chromatogr.*, **626**, 245, 1992.
57. M.G. Kahaledi, M.R. Hadjmohammadi, and B. Ye, *Anal. Chem.*, 1993
58. K. Otsuka, M. Kashihara, Y. Kawaguchi, R. Koike, T. Hisamitsu, and S. Terabe, *J. Chromatogr.*, **652**, 253, 1993.
59. T. H. Rasmussen, L. K. Goebel, and H. M. McNair, *J. Chromatogr.*, **517**, 549, 1990
60. C. Plamer, M. Khaled, and H. McNair, *JHRC*, **15**, 756, 1992.

- 61 D.C. Tickle, G.N. Okafo, P. Camilleri, R.F.D. Jones, and A.J. Kirby, *Anal. Chem.*, **66**, 4121, 1994.
- 62 J. Wang, I.M. Warner, *Anal. Chem.*, **66**, 3773, 1994.
- 63 J. Snopek, I. Jelinek, Z. Smolkov-Keulemansova, *J. Chromatogr.*, **609**,1, 1992.
- 64 Y. Tanaka, S. Terabe, *J. Chromatogr.*, **694**, 277, 1995.
- 65 H. Nishi, S. Terabe, *J. Chromatogr.*, **694**, 245, 1995.
- 66 J. Vindevogel, P. Sandra, "Introduction to Micellar electrokinetic Chromatography", Hüthig, Heidelberg, 1992.
- 67 M. G. Khaled, Handbook of Capillary Electrophoresis, J. P. Landers Eds. CRC press, 43, 1994.
69. R. Kuhn, S. Hoffsteter-Kuhn, Capillary Electrophoresis: Principles and Practice, Springer-Verlag, 1992, P 7.
70. S. Hjerten, M. D. Zhu, *J Chromatogr.*, **346**, 84, 1985.
- 71 S. Hjerten, J. Liao, K. Yao, *J. Chromatogr.*, **387**, 127, 1987.
72. S. Chen, J. E. Wiktorowicz, *Anal. Biochem.*, **206**, 84, 1992.
73. J. R. Mazzeo, I. R. Scrull, *Anal. Chem.*, **63**, 2852, 1991.
74. S. Hjerten, K. Elenbring, F. Kilar, J. L. Lias, A.J. C. Chen. C. J. Liebert, and M. Zhu, *J. Chromatogr.*, **403**, 47, 1987.
75. P. Bocek, P. Gebauer, V. Dolnik, and F. Foret, *J. Chromatogr.*, **334**, 157. 1985.
76. T. Hirokawa, A. Ohmori, Y. Kiso, *J. Chromatogr.*, **634**, 101, 1993.
77. F. Foret, E. Szoko, B. L.Karger, *J. Chromatogr.*, **608**, 3, 1992.
78. N. J..Reinoud, U. R. Tjaden, and J. van der Greef, *J. Chromatogr.*, **653**, 303, 1993.
79. K. W. Yim, *J. Chromatogr.*, **545**, 403, 1991.
80. M. Zhu, R. Rodringuez, T. Wehr, *J. Chromatogr.*, **559**, 479, 1991.
81. M. Zhu, D. L. Hansen, S. Burd, and F. Gannon, *J. Chromatogr.*, **480**, 311, 1989.
82. J. Koenig, Spectroscopy of Polymers, American Chemical Society, Washington, DC, 1992.
- 83 A. E. Tonelli, NMR Spectroscopy and Polymer Microstructure: The conformational connection, VCH, 1989.
- 84 A. Liebman, E. J. Levy, Pyrolysi and GC in Polymer Analysis, Chromatographic Science Series, Vol 29, Marcel Dekker, Inc., 1979.
- 84 S. A. Liebman, E. J. Levy, Pyrolysis and GC in Polymer Analysis, Chromatographic Science Series, Vol 29, Marcel Dekker, Inc., 1979, p 94.
- 85 J. K. Haken, *Adv. Chromatogr.*, **33**, 177, 1993.
86. C. Schwer, E. Kenndler, *Anal. Chem.*, **63**, 1801, 1991.
87. M. T. Bogert, R. R. Renshaw, *J. Am. Chem. Soc.*, **30**, 1140, 1908.
88. C. E. Stroog, *Prog. Polym. Sci.*, **16**, 561, 1991.
89. J. A. Cella, *Polymer Degrdaton and Stability*, **36**, 99, 1992.
90. M. E. Rogers, Synthesis and Characterization of High Performance Polyimide Homopolymers and Copolymers, Ph. D. Dissertation, VPI, 1993.

91. I. Y. Chang, Overview of Thermoplastic Compositions Technology, Du Pont Fibers and Composites, 1992.
92. T. Omote, K. Koseki, and T. Yamamoka, *Macromolecules*, **23**, 4788, 1990.
93. K. Matsumoto, P. Xu, *J. Appl. Polym. Sci.*, **47**, 1961, 1993.
94. Personal communication with Biao Tan.
95. H. F. Mark and G.S. Whitby, Eds. Collected papers of W. H. Carothers', Inter Science Publishing Company, New York, NY, 1940.
96. T. Satow, A. Machida, K. Funakushi, and R. Palmieri, *JHRC*, **14**, 276, 1991
97. C. F. Poole, W. F. Sye, S. Singhawangcha, F. Hsu, A. Zlatkis, A. Arfridsson and J. Pessman, *J. Chromatogr.*, **199**, 123, 1980..
98. Karl Blau and John Halker, Handerbook of Derivatives for Chromatography, 2nd Edition, John Wiley & Sons, pp 31-47.
99. K. Kawashiro, S. Morimoto and H. Yoshida, *Bull. Chem. Soc. Jpn.*, **58**, 1903, 1985.
100. Y. Wang, L. G. Enriquez, M. Bonilla and H. M. McNair, Picton' **95**, presentation 038, New Orleans.
101. Imai, K.; Toyo'oka, T. Selective Sample Handling and Detection in High Performance Liquid Chromatography. Frey, R.W., Zeck, K., Eds.; Elsevier: Amsterdam, 1988; pp 209-288.
102. Reaction Detection in Liquid Chromatography; Krull, I. S., Ed.; Marcel-Decker, Inc.: New York, 1987.
103. Y. Miyashita and S. Terabe, Beckman P/ACE System 2000 application Data, DS-767(1990). 3.2.11
104. B. L. Hogan, E.Y. Yueng, E.Y. *J. Chromatogr. Sci.* , **28**, 15-18, 1990.
105. J.W. Jorgenson, K. D. Lukcas, *Anal. Chem.*, **60** , 2642-2646, 1988.
106. J. Liu, K. A. Cobb, M. Novotny, *J. Chromatogr.*, **468** , 55-65, 1988.
107. M. Yu, N. J. Dovichi, *Anal. Chem.*, **61**, 37, 1989.
108. J. Liu, O. Shirota and M. Novotny, *Anal. Chem.*, **63** , 413, 1991.
109. Y. F. Cheng and N. J. Dovichi, *Science*, **242** , 562, 1988.
110. R. Samejima, *J. Chromatogr.* **96**, 250 , 1974.
111. M. Albin, R. Weinberger, E. Snapp and S. Moring, *Anal. Chem.*, **63** , 417, 1991.
112. N.A. Guzman, C. L. Gonzalez ect. Capillary Electrophoresis Technology; Norberto A. Guzman, Ed. Marcel Dekker, Inc. 1993, pp 643-672
113. S. Udenfriend, S. Stein, P. Böhlen, W. Dairman, W. Leimgruber and M. Weigele, *Science* . **178**, 871, 1972.
114. H. Vorbrüggen, *Angew. Chem.*, Int. Ed. Engl., **2**, 211, 1963.
115. E.J. Corey and A. Venkateswarlu, *J. Am. Chem. Soc.*, **94**, 4013, 1972.
116. J. J. Myher, A. Kuksis, L. Marai and S. K. F. Yeung, *Anal. Chem.*, **50**, 557 1978.
117. H. D. Durst, M. Milano, E. J. Kikta, Jr., S. A. Conelly and E. Grushka, *Anal. Chem.*, **47**, 1797, 1975.
118. W. Distler, *J. Chromatogr.*, **312**, 461, 1984.
119. P. H. Zoutendam, P.B. Bowman, T. M. Ryan and J. L. Rumph, *J. Chromatogr.*, **283**, 281, 1991.

120. H. C. Jordi, *J. Liq Chromatogr.*, **1**, 215, 1978.
121. B.F. Kenney, *J. Chromatogr.*, **546**, 423, 1991.
122. X. Huang, J.A. Luckey, M.J. Gordon and R.N. Zare, *Anal. Chem.*, **61**, 766, 1989.
123. C.L. Ng, H.K. Lee and S.F.Y. Li, *J. Chromatogr. Sci.*, **30**, 167, 1992.
124. R. J. M. Vervoort, F. A. Maris, and H. Hindriks, *J. Chromatogr.*, **623**, 207, 1992.
125. W. Thormann, S. Lienhard, P. Wernly, *J. Chromatogr.*, **636**, 137, 1993.
126. P. Wernly, W. Thormann, *Anal. Chem.*, **63**, 2878, 1991.
127. C. Sun, *Yaowu Fenxi Zazhi*, **13**, 48, 1993.
128. G. L. Chee, T. S. M. Wan, *J. Chromatogr.*, **612**, 172, 1993.
129. K. D. Altria, *LC-GC. Int.* **6**, 616, 1993.
130. L. A. Berrueta, B. Gallo, F. Vicente, *Chromatographia*, **40**, 474, 1995.
131. Product Information #4041247 on Zantac[®] (Ranitidine Hydrochloride), Glaxo Pharmaceuticals, RTP, NC, 1992.
132. E. K. Korchemmaya, A. N. Ermakov, and L. P. Bochkova, *J. Anal. Chem., USSR (Engl. Transl.)*, **33**, 635, 1984
133. S. Fujiwara, S. Honda, *Anal. Chem.*, **59**, 487, 1987.
134. S. Naylor, L. M. Benson, and A. J. Tomlinson, in CRC Handbook of Capillary Electrophoresis-A Practical Approach, J. P. Landers, Ed. (CRC Press Inc. 1992, p 459
135. Y. Walbroehl, J.W. Jorgenson, *J. Chromatogr.*, **315**, 135, 1984.
136. S. S. Rachhpal, M.G. Khaledi, *Anal. Chem.*, **66**, 1141, 1994
137. A.J. Tomlinson, L.M. Benson, and S. Naylor, *LC-GC*, **12**, 122, 1994)
138. H. Salimi-Moosavi, R.M. Cassidy, *Anal. Chem.*, **67**, 1067, 1995
139. M.G. Kahaledi, B. Ye, F. Wang, and V. Ward, # 124, 17th International Symposium on Capillary Chromatography and Electrophoresis, Wintergreen, VA, May 7-11, 1995.
140. G.N.W. Leung, T.S.M. Wan, # 147, 17th International Symposium on Capillary Chromatography and Electrophoresis, Wintergreen, VA, May 7-11, 1995.
141. CRC Handbook of Chemistry and Physics, L.R. David, Ed., 75th Edition.
142. M. Y. Khaled, Selectivity and Detection in Capillary Electrophoresis, Ph. D. Dissertation, VPI, 1994.

VITAE

Xiaowei Sun was born on September 29, 1963 in Zhejiang Province, China. In August, 1984, he obtained a Bachelor of Science Degree in Chemistry from Fudan University in Shanghai, China. After graduation, he worked as a teacher at Shanghai University of Science and Technology for six years and as a research assistant at Shanghai Institute of Organic Chemistry for a year. He entered the graduate program with teaching assistantship at Virginia Polytechnic Institute and State University in August, 1991, and studied analytical chemistry under the guidance of professor Harold McNair. He held summer internship at S.C. Johnson Wax in 1993 for pesticides and personal care products analyses. He is a member of the American Chemical Society (ACS).

A handwritten signature in black ink that reads "Xiaowei Sun". The signature is written in a cursive, flowing style and is positioned diagonally on the page.